



Chemistry A European Journal

 **Chemistry
Europe**
European Chemical
Societies Publishing

Accepted Article

Title: Geodesic–Planar Conjugates: Substituted Buckybowls –
Synthesis, Photoluminescence and Electrochemistry

Authors: Johannes Bayer, Jan Herberger, Lukas Holz, Rainer Winter,
and Thomas Huhn

This manuscript has been accepted after peer review and appears as an Accepted Article online prior to editing, proofing, and formal publication of the final Version of Record (VoR). This work is currently citable by using the Digital Object Identifier (DOI) given below. The VoR will be published online in Early View as soon as possible and may be different to this Accepted Article as a result of editing. Readers should obtain the VoR from the journal website shown below when it is published to ensure accuracy of information. The authors are responsible for the content of this Accepted Article.

To be cited as: *Chem. Eur. J.* 10.1002/chem.202003605

Link to VoR: <https://doi.org/10.1002/chem.202003605>

WILEY-VCH

Geodesic–Planar Conjugates: Substituted Buckybowls – Synthesis, Photoluminescence and Electrochemistry

Johannes Bayer[‡], Jan Herberger[‡], Lukas Holz, Rainer Winter and Thomas Huhn^{*[a]}

^[a] J. Bayer, J. Herberger, L. Holz, Prof. Dr. R. Winter and Dr. T. Huhn

Fachbereich Chemie, Universität Konstanz, Universitätsstr. 10, D-78457 Konstanz, Germany

Tel: (+49)7531 - 88 2283; Fax: (+49) 7531-884424

*E-mail: thomas.huhn@uni-konstanz.de

[‡] Equal contribution

Abstract

C–C Cross coupling products of bowl-shaped *as*-indaceno[3,2,1,8,7,6-*pqrstuv*]picene (Idpc) and different planar arenes and ethynyl-arenes were synthesized. Photoluminescence as well as electrochemical properties of all products were investigated and complemented by time-dependent quantum chemical calculations. UV/vis- spectroelectrochemistry investigations of the directly linked (Idpc)₂ uncovered the formation of 65 % (Idpc^{•-})₂ as the major reduction product. All coupling products showed fluorescence. Ferrocene-1-yl-Idpc was structurally characterized by X-ray diffraction and is a rare example of a ferrocene-containing buckybowl exhibiting luminescence.

Introduction

Indacenopicene (Idpc) is one member of the interesting class of condensed polyarenes with a non-planar π -surface. The curvature of these open geodesic molecules results from substituting some of the six-membered rings within their poly-benzenoid network by five-membered ones. Some of these bowl-shape molecules can be mapped on the surface of buckminsterfullerene, hence they are often named “bucky-bowls”. Corannulene (CA) as the most studied member of this class of compounds was already synthesized in 1966.^[1]

The non-planarity of geodesic arenes, such as CA, benzocorannulene or indenocorannulene, imposes novel physical properties^[2-5] and chemical reactivity,^[6-7] which sets them apart from planar polycyclic aromatic hydrocarbons (PAHs). The most distinct feature is the inherent presence of a dipole moment, thus allowing formation of dipolar structures in the solid state.^[8] As a direct consequence of the pyramidalization of carbon atoms, the π -bonds are weakened, i.e. LUMO is lowered and HOMO is raised in energy, approaching towards the state without conjugation. A second aspect to consider is the mixing of s-orbital character with the p-orbital of the π -bond, thus lowering the energy of both, the

HOMO and the LUMO. As a net effect the HOMO energy remains virtually unchanged while the LUMO is substantially lowered in energy.^[9] Therefore, these molecules can be easily reduced offering potential applications in electron storage and electroluminescence applications.^[10-11]

During the last decades the chemistry and physics of CA-derived bucky-bowl derivatives was thoroughly studied.^[12-18] However, comparably less work has been carried out in the field of Idpc and its derivatives. The first synthetic approach towards Idpc by palladium catalyzed cyclization of suitable precursors was reported already in 2000 but lacked generality.^[19] The aluminium-oxide mediated cove-region ring-closure through C–F bond activation of fluoroarenes^[20] towards pristine Idpc and other bowl-shape PAHs developed by Amsharov *et al.* in 2012 constituted a major breakthrough.^[21] A comparative study of the fundamental aromaticity and electrochemistry of unsubstituted Idpc and CA revealed a lower delocalization of electrons in Idpc compared to other PAHs as a direct result of the nonequivalence of the five six-membered rings. The low LUMO energy and the smaller HOMO–LUMO gap compared to CA, render Idpc a particularly interesting π -acceptor for organic electronics.^[22] Bromine atoms at the periphery of an Idpc precursor were recently shown to be tolerated by the aluminum-oxide ring-closing methodology, but no C–C coupling reactions on Idpc were reported yet.^[23]

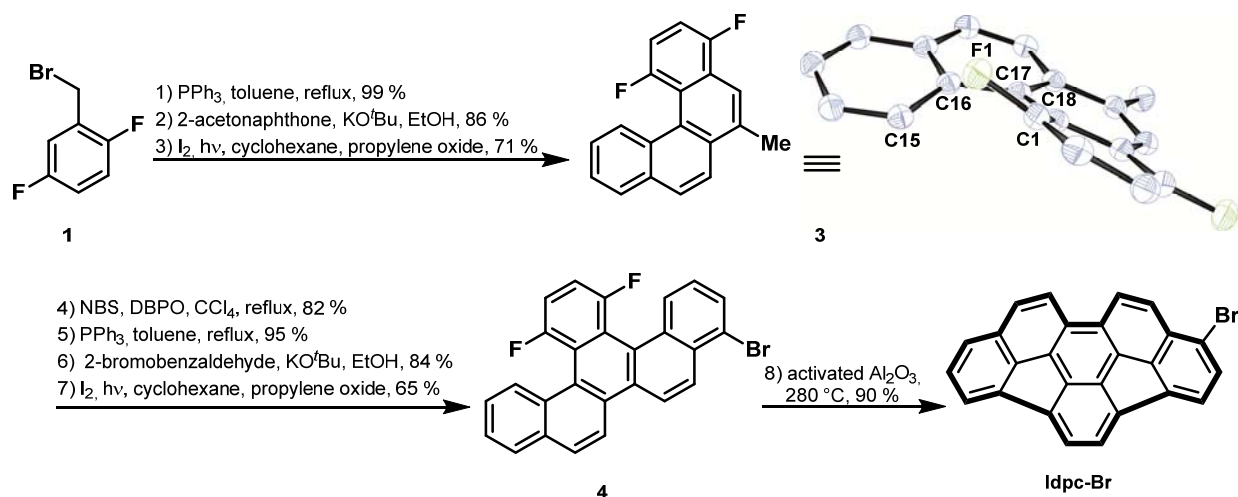
The present study aimed at exploring the scope of **Idpc-Br** functionalization by cross-coupling reactions with a panel of differently substituted phenyl boronates as well as phenyl acetylenes, both electron-rich and electron-deficient. Electronic absorption spectra as well as fluorescence emission spectra and cyclic voltammograms of the resulting bowl-shaped Idpc–arene and Idpc–ethynyl-arene hybrid materials were obtained. The results of these studies are discussed together with those of accompanying quantum chemical calculations on the DFT-level.

Results and Discussion

Synthesis and solid state structure

1-Bromoindacenopicene (**Idpc-Br**) served as the common starting material for all Suzuki and Sonogashira coupling reactions towards Idpc–(ethynyl)arene hybrid materials. **Idpc-Br** was synthesized by thermal aluminum oxide promoted dehydrofluorination of neat 4-bromo-13,16-difluorobenzo[*s*]picene (**4**) at 280 °C in a sealed tube.^[23] The above picene **4** is accessible from a sequence of two consecutive Wittig and oxidative photocyclization reactions starting from 2,5-difluorobenzyl bromide (**1**) (**Scheme 1**). An *E/Z*-mixture of stilbene **2** obtained from the Wittig reaction of 2-acetonaphthone was subjected to a Mallory photocyclization^[24] to afford 1,4-difluoro-6-methylbenzo[*c*]phenanthrene (**3**), a substituted [4]helicene. Single crystals suitable for an X-ray diffraction study could be grown by slow evaporation of a saturated solution of phenanthrene **3** in

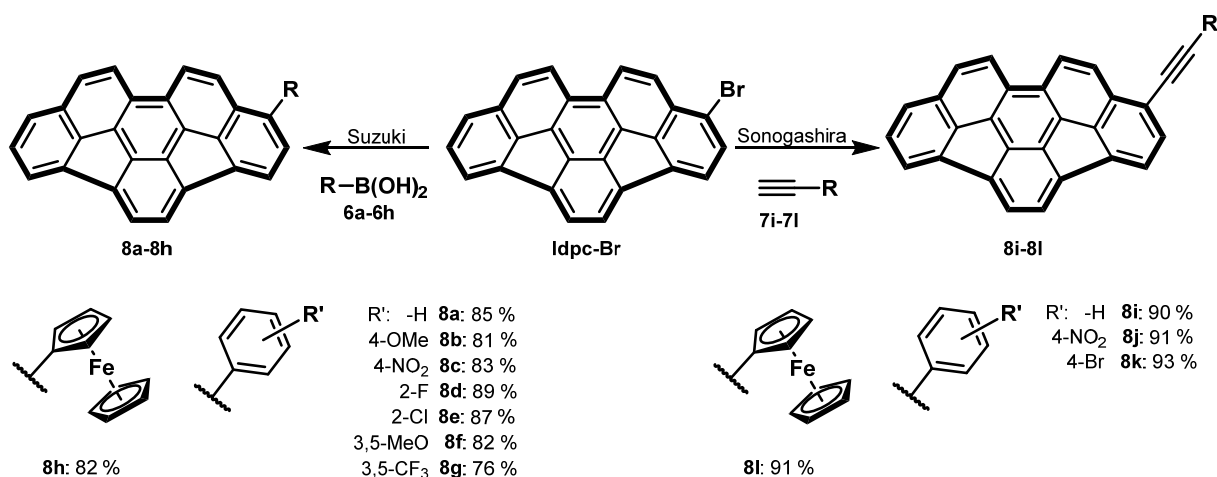
dichloromethane. **3** crystallizes in the monoclinic space group $P2_1/n$ with a single molecule forming the asymmetric unit. The unit cell consists of four molecules with no additional solvent. The structure is best characterized as helically-bent with an angle of 26.67° between the two planes described by the 10 atoms of each naphthalene subunit. The torsion angles C1–C18–C17–C16 and C15–C16–C17–C18 of 27.19° and 21.08° at the inner helical rim are much larger than in the parent [4]helicene [CSD code: BZPHAN] (17.11° and 20.16°), as is the dihedral angle of 37.45° between both terminal benzene rings when compared to that of 27.26° for [4]helicene (**Scheme 1**). Both naphthalene subunits in **3** are themselves severely bent from planarity as a result of the strong steric repulsion between the C1–F and the C15–H atoms which are only 2.297 Å apart. A further consequence of the difluoro substitution pattern is found in the packing of the difluoro [4]helicene **3** in the solid state. It adopts a partial face-to-face arrangement of the fluorine-rich parts of the molecules with alternating layers of the individual enantiomers (**Figure S4/S5**) and alternating interlayer distances of 3.381 Å and 3.610 Å. This contrasts to the solid structure of [4]helicene, which is characterized by the archetypical herringbone edge-to-face arrangement.^[25] The synthesis of the planar bucky-bowl precursor 4-bromo-13,16-difluorobenzo[*s*]picene (**4**) of **Idpc-Br** was then completed by a sequence of benzylic bromination, Wittig reaction with 2-bromobenzaldehyde and a second Mallory photocyclization.



Scheme 1. Synthesis of 1-bromoindacenopicene (**Idpc-Br**); inset shows ORTEP of precursor 1,4-difluoro-6-methylbenzo[*c*]phenanthrene (**3**), hydrogen atoms are omitted for clarity, ellipsoids are drawn at the 50% probability level.

With the 4-bromo-13,16-difluorobenzo[*s*]picene (**4**) available a first test towards further functionalization was undertaken by Stille coupling with tris-*n*-butylstannylderrocene. Gratifyingly, this provided 4-ferrocenyl-13,16-difluorobenzo[*s*]picene (**5**) in 65 % yield. Dark red single crystals were grown by slow diffusion of *n*-pentane into a saturated solution of **5** in dichloromethane. **5** crystallizes in the monoclinic space group $P2_1/n$ with a single molecule forming the asymmetric unit.

The difluoro-substituted phenyl ring is severely bent out of the picene plane (**Figure S6**). The rather short fluorine...hydrogen distances C4H...F1 (2.382 Å) and C15H...F2 (2.362 Å) should make the molecule ideally suited for the aluminum oxide promoted dehydrofluorination reaction. However, the latter reaction failed irrespectively of reaction time and temperature. Even at temperatures as high as 400 °C and reaction times of more than 120 min, only unchanged starting material was recovered. Fortunately, its bromo-substituted precursor **4** could be smoothly dehydrofluorinated to provide **Idpc-Br** in an excellent yield of 90 % upon conventional heating for less than 120 min neat on preactivated aluminum oxide to 280 °C.



Scheme 2. Overview over hybrid-structures accessed by cross coupling **Idpc-Br** with a selection of differently substituted boronates **6a-h** and alkynes **7i-l**.

With **Idpc-Br** in hands, Suzuki and Sonogashira cross-coupling reactions with a variety of differently substituted phenyl boronates **6a-h** and phenylacetylenes **7i-l** were pursued (**Scheme 2**). Yields of Sonogashira couplings were generally higher (> 90 %) than those of the Suzuki couplings, which nevertheless still exceeded 80%, except for the case of *m*-CF₃-Ph (76%). The structures and chemical constitution of all new coupling products **8a-l** were confirmed by two-dimensional NMR techniques.

The structure of **Idpc-Fc** was additionally established by X-ray crystallography. Single crystals suitable for a diffraction study were grown by slow diffusion of *n*-hexane into a saturated dichloromethane solution at r.t. **Idpc-Fc** crystallizes as dark red tiny platelets in the orthorhombic space group *Pbca* with a single molecule in the asymmetric unit; the unit cell contains eight molecules. In contrast to parent Idpc^[21] [CSD code: FAWKIZ] and 9,12-dibromo-Idpc^[23] [CSD code: RARRUA], the only two other structurally characterized members of the Idpc-family,^[26] **Idpc-Fc** is chiral due to its monosubstitution in conjunction with the bowl shape of the Idpc-fragment; it crystallizes as a racemic mixture. The ferrocene adopts an *exo*-orientation with respect to the Idpc. The inter-ring torsion angle between the planes of the cyclopentadienyl and the adjacent phenyl ring of Idpc is 36.28°

and thus still permits efficient conjugation.^[27-28] The orientation of a molecule **Idpc-Fc** with respect to its neighboring molecules in the solid state is more complex than it is in the parent **Idpc**. The latter forms unidirectional, columnar superimposable, bowl-in-bowl stacks with a uniform bowl-to-bowl distance of 3.829 Å. In contrast **Idpc-Fc** forms pairs of columnar bowl-in-bowl stacks. The bowl-shaped **Idpc** rings within every pair of stacks share the same orientation whereas neighboring double stacks are mutually oriented in opposite directions. Individual pairs of columns are separated by double layers of ferrocenyl substituents (**Figure 1**). Within every column the individual enantiomers alternate along the longcolumn axis, which results in a twisted offset of every **Idpc**-moiety relative to its nearest neighbor (**Figure S8**). In consequence, only the Fc-bonded fluoranthene parts of the **Idpc** π -system do overlap (lower part of **Figure 1**). The four centroid-centroid distances between the three six- and the one five- membered rings of the two “fluoranthene”-layers vary only little at values of 3.721 to 3.795 Å (**Figure S10/11**). These distances are appreciable shorter than those in 9,12-dibromo **Idpc** (3.91 Å) and in the parent **Idpc** (3.829 Å), which is indicative of convex-concave interactions.^[29] The two C–C bonds of 1.529(9) Å (C3a–C3e) and 1.531(9) Å (C5a–C5e) formed during the defluorination step are by far the longest of the entire molecule and approach almost those of a typical C–C single bond, indicating a lack of conjugation.^[22] The bowl depth of 1.406 Å as measured from the centroid of the central picene ring and the plane defined by atoms C1-C3 and C6-C8 is slightly deeper than in the parent **Idpc** (1.334 Å). The π -orbital-axis vector (POAV) method is a direct measure of the curvature of bent π -systems.^{[30],[6]} The pyramidalization angle θ_p ($\theta_p = 90 - \theta_{\sigma\pi}$) is a direct measure of deviation from orthogonality of the σ - and π -orbitals at a certain carbon center. The values calculated based on the X-ray data of **Idpc-Fc** for the inner six carbon atoms range from 7.3° to 3.5° and are on average slightly larger than for unsubstituted **Idpc** (**Figure S12**). However, the difference is not significant and might originate from the different orientation of **Idpc-Fc** compared to parent **Idpc** in the crystal.

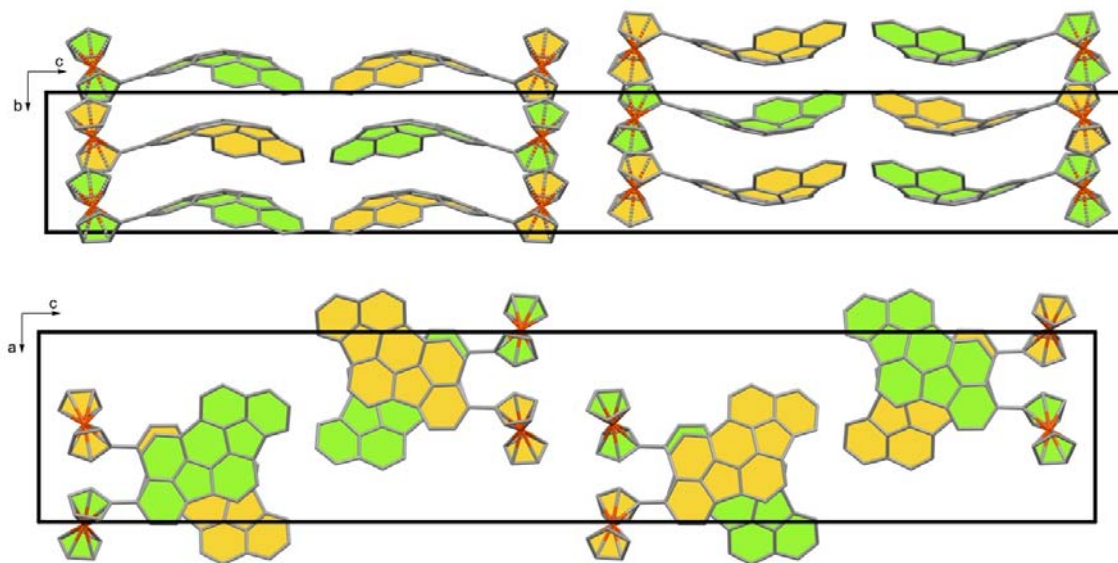
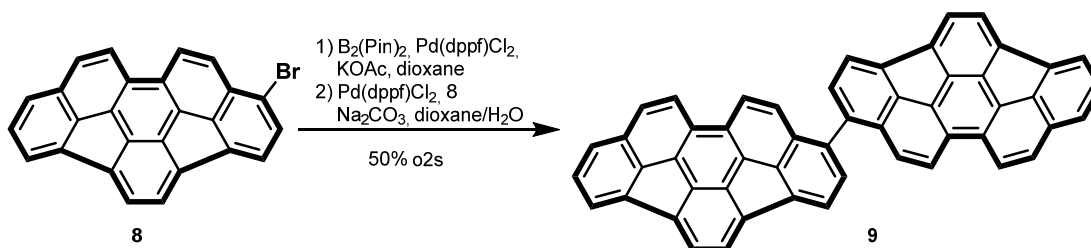


Figure 1. Packing diagram of **Idpc-Fc (8h)** in the crystal. Top: View along *a*-axis; Bottom: stacked view along *b*-axis; Enantiomers are shown in different colors, elementary cell shown in black.

The coupling products **8a-8h** resulting from Suzuki reactions are in general much more soluble in common organic solvents such as dichloromethane or tetrahydrofuran as compared to their Sonogashira counterparts **8i-8l** which are significantly less soluble, even in tetrachloroethane. In both series the Fc-derivatives are the ones with highest solubility. **Idpc-Br** is only sparingly soluble in dichloromethane, chloroform and THF. We were therefore interested to see if a coupling of two molecules **Idpc** could be achieved or if solubility issues would prevent this reaction. Borylation of **Idpc-Br** with bis(pinacolato)diboron under palladium catalysis proceeded smoothly in 1,4-dioxane and we were pleased to finally isolate a total yield of 50% of dimeric (**Idpc**)₂ over two steps (**Scheme 3**). This sets the stage for new inclusion complexes with other π -systems based on coupled indacenopicene moieties or molecular electronics with indacenopicene-based anchoring groups. However, the limited solubility of (**Idpc**)₂ might be a limiting factor.



Scheme 3. Synthesis of 1,1'-bisindacenopicene (**Idpc**)₂ via Suzuki coupling of **Idpc-Br** with *in situ* generated 1-pinacolatoboryl **Idpc (10)**.

Electronic absorption spectroscopy

The electronic absorption spectra of indacenopicene and its corresponding derivatives are characterized by an intense band at 250 nm – 300 nm, a structured band at 300 nm to 340 nm, which is merged into the low-energy flank of the former, a vibronically resolved transition at 350 nm – 400 nm, a series of poorly resolved, overlapping bands between 425 nm and 460 nm, as well as a very weak absorption feature at 460 nm to 530 nm. (*c.f.* **Figure 2** and **Table 1**).

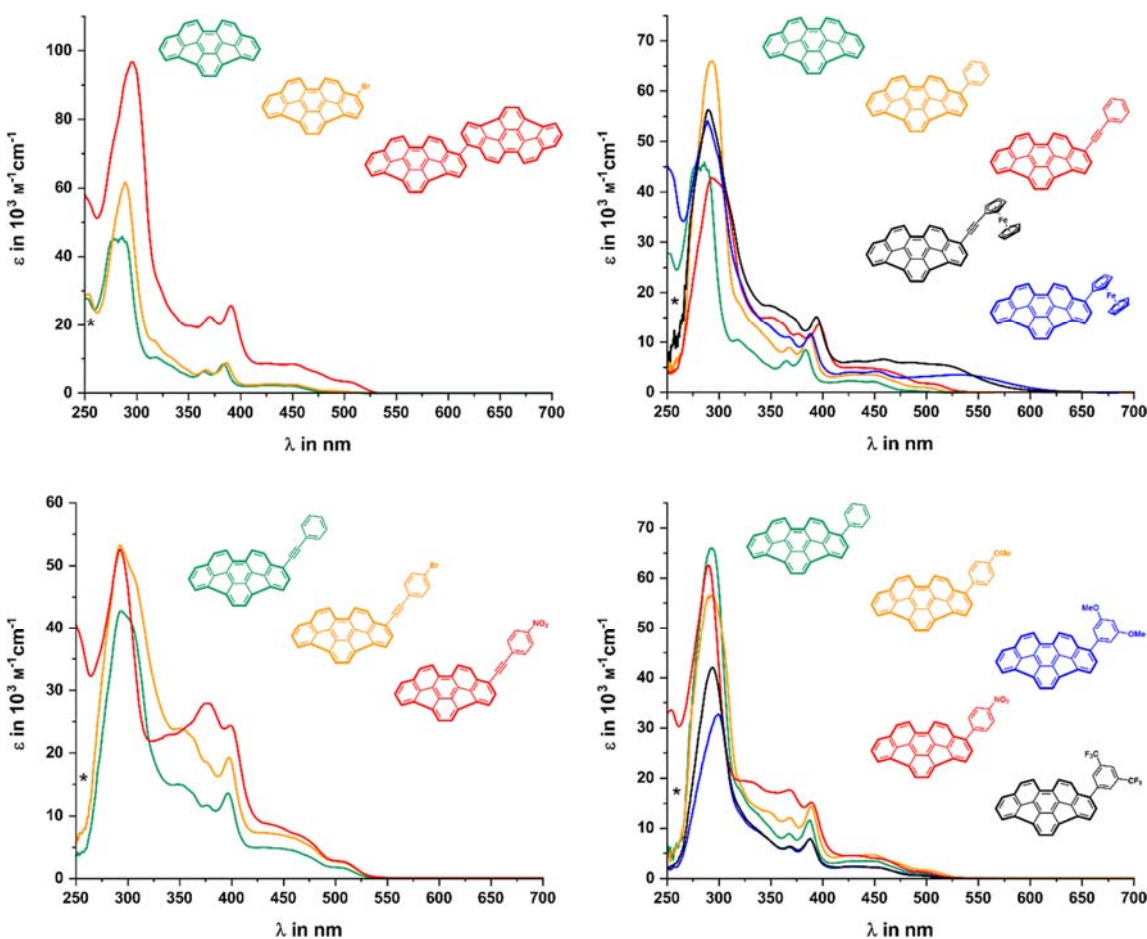


Figure 2. Electronic absorption spectra of indacenopicene and the new phenyl or phenylethynyl derivatives in dichloromethane.

Introduction of a phenyl or phenylethynyl substituent at the outer rim of indacenopicene leaves the general absorption features of the parent arene unchanged despite the lowering from C_s symmetry of **Idpc** to C_1 symmetry. However, hyperchromicity as well as a bathochromic shift of all bands are observed. The bathochromic shift follows the ordering $H < Br < Ph < Idpc \approx -\equiv-Ph$. Inductive effects as well as orbital interactions between the frontier orbitals of indacenopicene and the respective substituent, *i.e.* the increase of the extended π -system, contribute to this observation. DFT calculations

indicate that substitution generally affects the LUMO more than the HOMO, *i.e.* the magnitude of stabilization of the LUMO is greater than the destabilization of the HOMO. This holds true in particular for electron-neutral or electron-accepting substituents. Only for the electron donating anisyl and ferrocenyl substituents the HOMO is more destabilized than the LUMO (*c.f.* ESI). Introduction of a ferrocenyl or ethynylferrocenyl substituent results in a gain in intensity and a further bathochromic shift of the absorption bands and provides an additional broad absorption feature at 519 nm and 532 nm, respectively. Earlier studies on CA congeners yielded very similar results.^[31-35] Thus, Topolinski *et al.* studied the influence of ferrocenyl substituents linked *via* various spacers and found that the bathochromic shift increased along the ordering none < phenyl \approx ethynyl < vinyl < butadienyl owing to an increasing π -conjugation between the CA and the ferrocenyl pendant.^[35-36] Concerning **Idpc-Fc** and **Idpc \equiv -Fc** the stated trend is reversed. Presumably, the greater bowl depth of indacenopicene (*vide supra*) in comparison to CA imposes a more complex description of the electronic structure of these compounds. Interestingly, the benzannulated derivative of indacenopicene, where two indacenopicene moieties are fused *via* a joint aromatic ring, does not lower the energy of the electronic transitions as compared to our phenyl derivatives.^[21]

TD-DFT calculations were performed in order to further explore the electronic structure of these compounds. The five distinct electronic transitions defining the spectral envelope of parent **Idpc** can be assigned to $\pi\pi^*$ transitions between the highest three occupied and the three lowest unoccupied frontier orbitals (*c.f.* **Figure 3**). Interestingly, our computations discriminate between electronic transitions that involve the rings of higher (rings A, D, and E) and lower (rings B and C) π -electron delocalization.^[22] Taking this into account, the individual transitions can be described as follows: The transition at 491 nm (HOMO \rightarrow LUMO) is mainly centered at the ADE-rings. Next, at 449 nm, the H-1 \rightarrow LUMO transition involving intramolecular charge transfer (ICT) from the BC to ADE rings can be identified. The third transition at 384 nm (H-2 \rightarrow LUMO) is best described as a transition between orbitals that are evenly distributed over the entire indacenopicene π -system. The last two transitions located at 318 nm (HOMO \rightarrow L+1) and 286 nm (HOMO \rightarrow L+2) have again charge-transfer contributions. However, the direction of the ICT is reversed as compared to the band at lowest energy and occurs from the ADE to BC rings. Appending a phenyl or ethynylphenyl substituent introduces some additional ICT character to the transitions of **Idpc**, the direction of which depends on the electron-donating or -accepting properties of the latter. However, the energetically second lowest transition maintains its pure $\pi\pi^*$ character. Appending a ferrocenyl or ethynyl-ferrocenyl substituent augments the ICT with metal-to-ligand charge-transfer (MLCT) character, in particular for the transition at lowest energy. The vibronic resolution of the band at 390 nm to 360 nm indicates an only marginal dd^* or MLCT admixture to the underlying transition. The bands at even higher energy

display increasing MLCT contributions (*c.f.* ESI for a detailed assignment). Despite these MLCT contributions, changing the polarity of the solvent has only a minor influence on the band positions (*c.f.* **Figures S44-48**). Solvatochromic shifts are very similar to those for indacenopicene itself, showing that ICT contributions within the π -conjugated framework dominate over those introduced by the appended phenyl or phenylethynyl substituent.

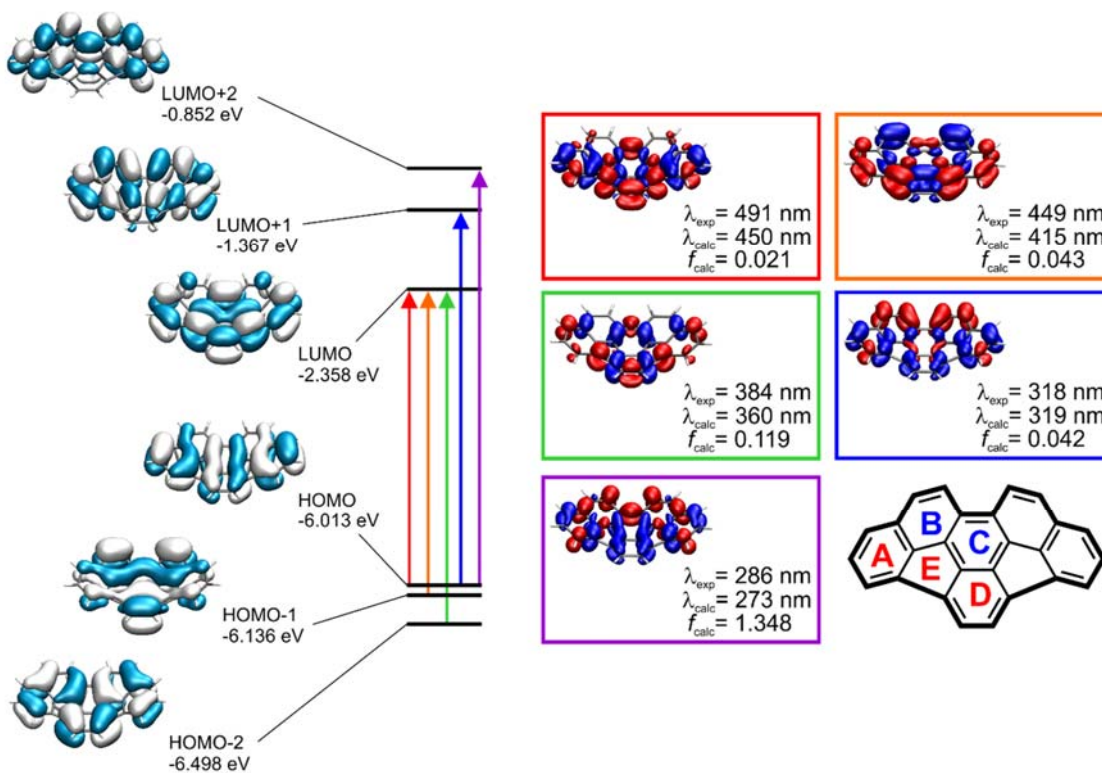


Figure 3. Frontier MOs of **Idpc** and corresponding electron density difference maps for individual transitions. Red color indicates an increase of electron density, and blue color a decrease of electron density.

Table 1. Absorption data of synthesized **Idpc** derivatives in dichloromethane.

Substance	λ in nm (ϵ in $10^3 \text{ M}^{-1} \text{ cm}^{-1}$)
Idpc	491 (0.30), 449 (2.17), 426 (2.25), 384 (8.48), 365 (6.30), 318 (10.5), 286 (45.9), 253 (27.8), 241 (32.5)
Idpc-Br	492 (0.60), 451 (2.49), 428 (2.67), 386 (8.83), 367 (6.77), 318 (15.3), 286 (61.7), 254 (29.0)
Idpc-Ph (8a)	498 (1.04), 449 (3.50), 429 (3.50), 387 (11.6), 368 (8.94), 336 (13.2), 319 (18.2), 293 (65.8)
Idpc-Ph-OMe (8b)	501 (1.60), 471 (3.15), 447 (4.79), 427 (4.51), 389 (14.4), 369 (11.9), 347 (13.3), 321 (18.7), 294 (56.6)
Idpc-Ph-NO ₂ (8c)	496 (1.37), 457 (4.00), 427 (4.51), 390 (15.2), 369 (17.6), 329 (19.3), 290 (62.5), 255 (33.7), 242 (37.1)
Idpc-Ph- <i>o</i> -F (8d)	494 (0.66), 451 (3.17), 429 (3.45), 387 (12.2), 368 (9.32), 336 (13.1), 320 (16.8), 294 (65.7)
Idpc-Ph- <i>o</i> -Cl (8e)	492 (0.14), 450 (2.39), 427 (2.68), 387 (10.3), 368 (7.62), 335 (10.9), 319 (13.9), 292 (61.1)
Idpc-Ph-(<i>m</i> -OMe) ₂ (8f)	499 (0.62), 451 (2.25), 427 (2.36), 388 (7.93), 369 (6.23), 347 (7.94), 334 (9.85), 322 (12.5), 299 (32.7)
Idpc-Ph-(<i>m</i> -CF ₃) ₂ (8g)	493 (0.59), 455 (2.17), 430 (2.47), 388 (7.83), 368 (6.42), 338 (9.59), 317 (15.2), 294 (42.1)
Idpc-Fc (8h)	532 (3.58), 452 (4.16), 428 (3.99), 389 (11.8), 367 (11.2), 346 (13.6), 317 (24.7), 290 (54.1), 255 (44.2), 247 (46.7)
Idpc≡-Ph (8i)	508 (1.65), 449 (4.75), 397 (13.6), 377 (11.7), 352 (14.8), 304 (40.6), 292 (42.6)
Idpc≡-Ph-NO ₂ (8j)	507 (2.73), 464 (6.86), 437 (8.64), 399 (24.3), 376 (28.0), 339 (22.9), 292 (52.4), 248 (41.2)
Idpc≡-Ph-Br (8k)	504 (2.68), 460 (6.45), 435 (7.24), 397 (19.3), 376 (18.6), 364 (22.1), 353 (23.7), 309 (46.4), 293 (53.2)
Idpc≡-Fc (8l)	519 (5.41), 485 (5.87), 459 (6.58), 432 (6.22), 394 (15.2), 373 (14.9), 350 (17.4), 311 (36.8), 290 (56.4)
(Idpc) ₂ (9)	504 (3.44), 474 (6.03), 452 (8.32), 425 (8.62), 391 (25.7), 370 (22.4), 351 (19.6), 322 (31.5), 296 (96.6), 254 (56.4), 244 (61.7)
(Idpc ²⁻) ₂	956 (2.46), 862 (4.24), 758 (7.22), 715 (7.47), 648 (8.61), 509 (6.82), 453 (10.8), 391 (27.1), 371 (29.1)

Luminescence spectroscopy

As discussed above the electronic absorption processes in indacenopicene derivatives have $\pi\pi^*$ character with varying degrees of ICT admixture. Photoexcitation of any derivatives at wavelengths down to 300 nm resulted in fluorescence, which is characterized by a vibrationally poorly resolved emission band (*c.f.* **Figure 4** and **Table 2**). In all cases, the emission originates from the S_1 state located at the Idpc moiety. Luminescence measurements carried out at 77 K in a glassy matrix of 2-methyl-tetrahydrofuran do not reveal any phosphorescence emission, in contrast to what was observed for CA.^[4]

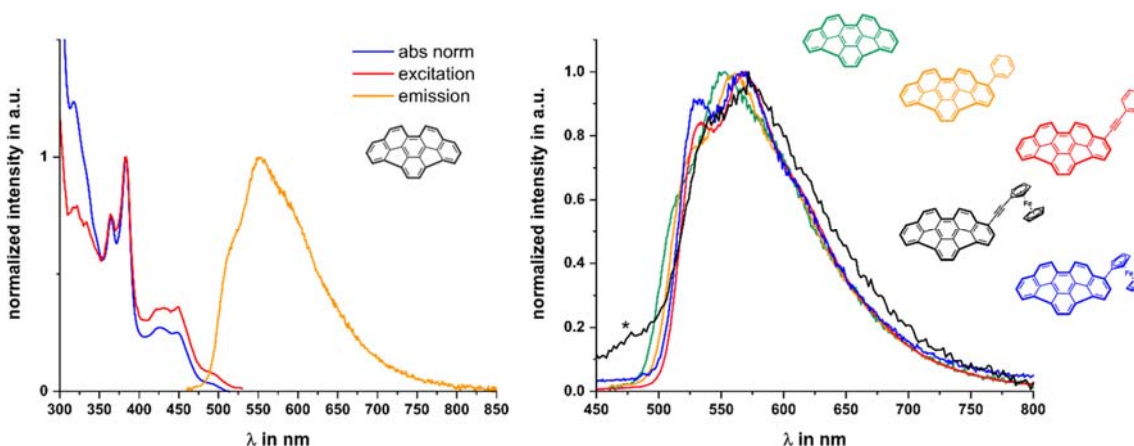


Figure 4. Left: superimposed absorption, excitation and emission spectra of **Idpc**. Right: superimposed emission spectra of representative derivatives of the new Idpc's measured in dichloromethane at room temperature.

In the series CA, cyclopentacorannulene, indenocorannulene, and indacenopicene the bowl depth increases from 0.877 Å, to 1.05 Å and 1.07 Å, and finally to 1.35 Å.^[37-40] Earlier studies on CA derivatives revealed that an increasing bowl depth goes in parallel with a decreasing quantum yield, e. g. from 0.07 for CA to 0.007 for indenocorannulene.^[2, 41-42] It was reasoned that the superior rigidity of the congeners is counterbalanced and even overcompensated by the introduced structural strain, thus opening nonradiative internal conversion pathways.^[2, 41] Furthermore, photophysical studies on indenocorannulene derivatives with flat aromatic appendages indicate that the emissive state is located at flat areas of the geodesic polyarenes, thereby bypassing detrimental structural rearrangement.^[41]

With this in mind the following statements concerning our new derivatives can be made: The low quantum yields of the Idpc's ($\Phi = 0.01$) adhere to the above-mentioned trend for the series of curved CAs. Extending the π -system by attachment of a peripheral aryl substituent increases k_r along the series **Idpc** < **Idpc-Ph** < **Idpc≡Ph** whereas k_{nr} remains rather unchanged, thus improving the respective quantum yields. Furthermore, the excited state life-times and Stokes shifts remain constant at circa 4 ns and 2300 cm^{-1} , respectively. The latter in combination with the invariant band shape

indicate that the excited state is located on the indacenopicene moiety. The time constant for non-radiative decay k_{nr} remains largely constant at approximately $2.4 \times 10^8 \text{ s}^{-1}$, irrespective of whether electron-donating or -withdrawing substituents are present at the aryl pendent. This indicates that all derivatives share a common deactivation pathway. Whereas modification of the phenyl-substituted derivative hardly influences k_r and Φ , introducing an ethynyl spacer increases Φ and boosts k_r by one order of magnitude. Fusing two indacenopicenes in (Idpc)₂ (**9**) increases Φ and k_r by a factor of four. However, using ferrocene or ethynyl ferrocene as substituent has no effect on k_r or on Φ as compared to parent **Idpc**. To the best of our knowledge, compounds **8h** and **8l** constitute the first ferrocene derivatives of indacenopicene and are the first geodesic polyarenes containing ferrocene or ethynyl ferrocene to exhibit luminescence.^[35-36, 43] Normally, ferrocene acts as a potent quencher of the excited states, either by energy transfer or electron transfer, followed by relaxation and the release of thermal energy.^[44] It is reasonable to assume that the ferrocene pendants are electronically decoupled in the excited state, thus inhibiting quenching processes. This assumption is further supported by inspection of the absorption and the excitation spectrum of Idpc-Fc (**8h**). Whereas irradiation into every absorption feature leads to emission from the energetically lowest excited state, the excitation spectrum clearly shows that the energetically lowest transition, which, according to quantum chemical calculations, has a strong contribution from molecular orbitals localized at the ferrocene nucleus, does not contribute to the emissive state (see ESI). In a very recent paper Kasprzak et al. reported on a tris(ferrocenylmethidene)sumanene showing a sumanene based luminescence.^[45]

Table 2. Photophysical data of **Idpc** and the new Idpc derivatives in dichloromethane solutions at room temperature.

Substance	λ_{max} in nm	Stokes shift in cm^{-1}	$\Phi^{\text{a)}$	$\tau_{1/2}$	k_r in 10^6 s^{-1}	k_{nr} in 10^8 s^{-1}
Idpc	553	2283	0.01	3.69±0.02	2.711	2.684
Idpc-Br	557	2372	0.01	3.82±0.07	2.617	2.591
Idpc-Ph (8a)	561	2255	0.03	4.08±0.02	7.357	2.379
Idpc-Ph-OMe (8b)	568	2354	0.02	4.76±0.02	4.199	2.057
Idpc -Ph-NO ₂ (8c)	560	2304	0.03	4.32±0.02	6.944	2.245
Idpc -Ph- <i>o</i> -F (8d)	556	2257	0.03	4.04±0.02	7.419	2.399
Idpc -Ph- <i>o</i> -Cl (8e)	554	2275	0.04	3.65±0.02	10.96	2.630
Idpc-Ph-(<i>m</i> -OMe) ₂ (8f)	560	2183	0.04	4.11±0.02	9.728	2.335
Idpc-Ph-(<i>m</i> -CF ₃) ₂ (8g)	557	2331	0.04	3.78±0.02	10.57	2.537
Idpc-Fc (8h)	566	2332	0.01	4.02±0.02	2.490	2.465
Idpc≡-Ph (8i)	568	2079	0.1	3.93±0.02	25.45	2.291
Idpc≡-Ph-NO ₂ (8j)	568	2118	0.08	3.58±0.02	22.33	2.568
Idpc≡-Ph-Br (8k)	568	2236	0.06	3.74±0.02	16.06	2.516
Idpc≡-Fc (8l)	572	2517	0.01	4.21±0.05	2.378	2.354
(Idpc) ₂ (9)	568	2236	0.04	3.98±0.02	10.06	2.414

^{a)} Absolute quantum yields are determined utilizing an integrating sphere.

Electrochemistry

Geodesic polyarenes are well known for their ability to be reduced by one or more electrons. Several studies were devoted to examining their electrochemical properties as well as the structures of the corresponding reduced forms as their alkali and alkaline earth salts.^[22, 46] Whereas CA can be reversibly reduced by up to four electrons, indacenopicene only displays two reversible one electron reductions. This is the consequence of the symmetry lowering from C_{5v} to C_s and the concomitant lifting of the degeneracy of the first two lowest unoccupied molecular orbitals.^[22]

Cyclic voltammetry was employed in order to investigate the influence of the various substituents on the reduction potentials of the new indacenopicenes (for experimental voltammograms see the ESI). The results of our studies on the new Idpc derivatives **8a-8k** in 1,2-dichlorobenzene/NBu₄PF₆ (0.1M) as the supporting electrolyte are summarized in **Figure 5** and **Table 3**. The cyclic voltammograms are characterized by two chemically mostly reversible reduction processes. Half-wave potentials of both redox events are strongly influenced by the substituents on the appended phenyl ring and spread over a range of more than 400 mV, such that the separation between the half-wave potentials of the first and the second reduction remains relatively constant at ca. 280 mV to 320 mV. The most anodically shifted potentials are observed for the nitro derivatives **8c,j** while those of the 4-anisyl and ferrocenyl derivatives **8f,h** closely resemble those of parent **Idpc**. This substituent effect reconfirms that the appended phenyl or phenylethynyl substituent have a strong bearing on the energies of the lowest

unoccupied frontier MOs, similar to what has been observed for their CA congeners^[5, 35-36, 47-48] and in agreement with the results of our quantum chemical studies. The three pairs of compounds of the phenyl and ethynylphenyl series with identical substituents on the phenyl ring (H in **8a,i**, NO₂ in **8c,j**, ferrocenyl in **8h,l**) indicate that the ethynyl spacer induces an anodic shift of ca. 100 mV. The same also holds for the Fe-centered reversible one-electron oxidation of the latter two ferrocene derivatives. The half-wave potentials of the ferrocene oxidation closely resemble that observed in ethynylferrocene-appended CA, which oxidizes at 130 mV.^[35]

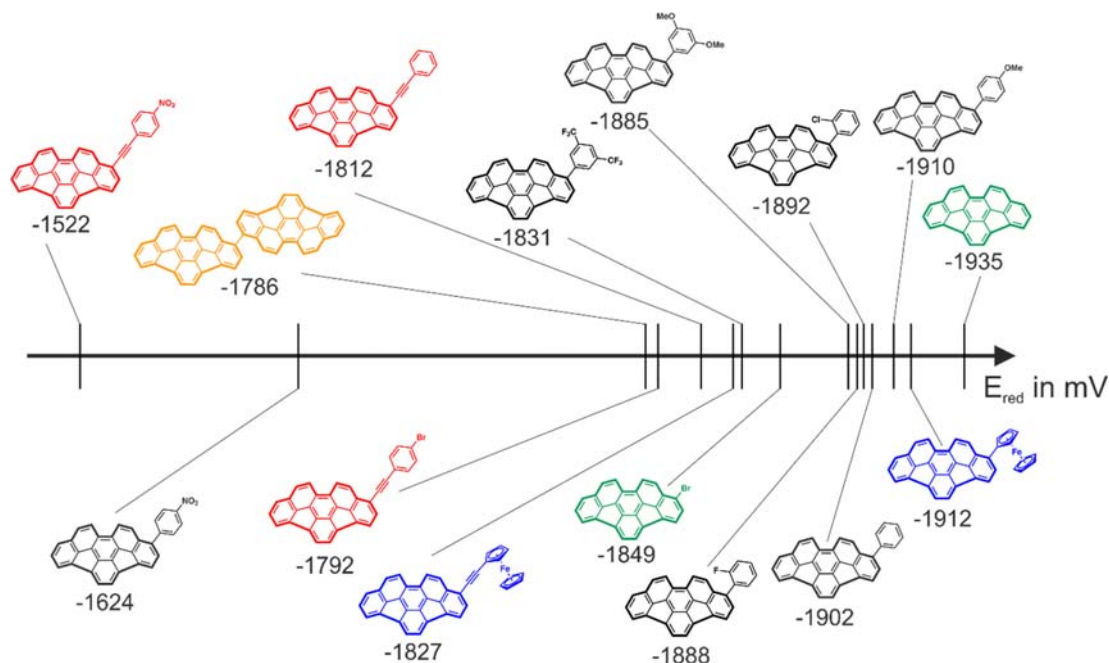


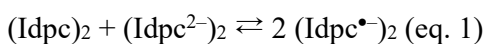
Figure 5. Graphical representation of the first reduction potential of the studied Idpc derivatives.

Table 3. Half-wave potentials of the indacenopicene derivatives in 1,2-dichlorobenzene/ NBu₄PF₆ (0.1M) in mV. Potentials are provided relative to the ferrocene/ferrocenium redox standard set at E_{1/2} = 0.000 V.

Compound	E _{1/2} 0/-	E _{1/2} 0/-2	ΔE _{1/2} relative to Idpc
Idpc	-1935	-	0
Idpc-Br	-1849	-	86
Idpc-Ph (8a)	-1902	-2221	33
Idpc-Ph-OMe (8b)	-1910	-2242	25
Idpc -Ph-NO ₂ (8c)	-1624	-1824	311
Idpc -Ph- <i>o</i> -F (8d)	-1888	-2224	47
Idpc-Ph- <i>o</i> -Cl (8e)	-1892	-2232	43
Idpc-Ph-(<i>m</i> -OMe) ₂ (8f)	-1885	-2202	50
Idpc-Ph-(<i>m</i> -CF ₃) ₂ (8g)	-1831	-2107	104
Idpc-Fc (8h) ^{a)}	-1912	-2248	23
Idpc≡-Ph (8i)	-1812	-2113	123
Idpc≡-Ph-NO ₂ (8j)	-1522	-1743 (-2180)	413
Idpc≡-Ph-Br (8k)	-1792	-2092	143
Idpc≡-Fc (8l) ^{b)}	-1827	-2147	108
(Idpc) ₂ (9)	-1786/-1858 ^{c)}	-2241	149

^{a)} Oxidation potential of **8h** at 68 mV. ^{b)} Oxidation potential of **8l** at 142 mV. ^{c)} The two first reductions of (Idpc)₂ (**9**) as obtained by square wave voltammetry.

In directly linked (Idpc)₂ (**9**) the first reductions of the individual picenes occur in a consecutive manner with a redox splitting ΔE_{1/2} of 72 mV. Such behavior entirely results from electrostatic interactions which is supported by UV/vis-SEC (spectroelectrochemistry) experiments in an optically transparent thin-layer electrochemical (OTTLE) cell.^[49] Upon slowly traversing the convoluted 0/- and -/2- reductions we observe the growth of low energy absorption bands with peaks/shoulders at 648 nm, 715 nm, 758 nm, and 956 nm, which resemble those in the 360 nm to 500 nm range of neutral Idpc's with respect to their pattern and shapes (see **Figure 6** and **Table 1**). The close similarity to the known absorptions of the corannuleny radical anion^[50] let us assign these features to the monoreduced (Idpc^{•-})₂; i.e. each individual Idpc unit of (Idpc)₂ was monoreduced. Most importantly, however, we do not observe any specific absorption of the mixed-valent radical anion (Idpc²⁻)(Idpc) at any point of the electrolysis. According to the ΔE_{1/2} value of 72 mV and the derived equilibrium constant of 17.7 for the ensuing comproportionation equilibrium (see equations 1 and 2),^[51] (Idpc^{•-})₂ represents the major species (64.6 %, with 17.7 % of (Idpc)₂ and (Idpc²⁻)₂ each) halfway along the electrolysis, i. e. after uptake of one electron per Idpc moiety of (Idpc)₂.



$$\ln(K_c) = F \cdot \Delta E_{1/2} / (R \cdot T) \text{ (eq. 2)}$$

In equation (2) *F* is the Faraday constant, *R* is the universal gas constant, *T* is the absolute temperature, and ΔE_{1/2} is the difference of half-wave potentials of the first- and second reductions in Volt.

Our failure to observe any additional absorption band at even lower energy as it would be typical of an intramolecular electron transfer transition in an electronically coupled mixed-valent species therefore indicates that the two Idpc subunits of $(\text{Idpc}^{\bullet-})_2$ remain electronically decoupled from each other and, hence, that the half-wave potential splitting is due to merely electrostatic interactions.

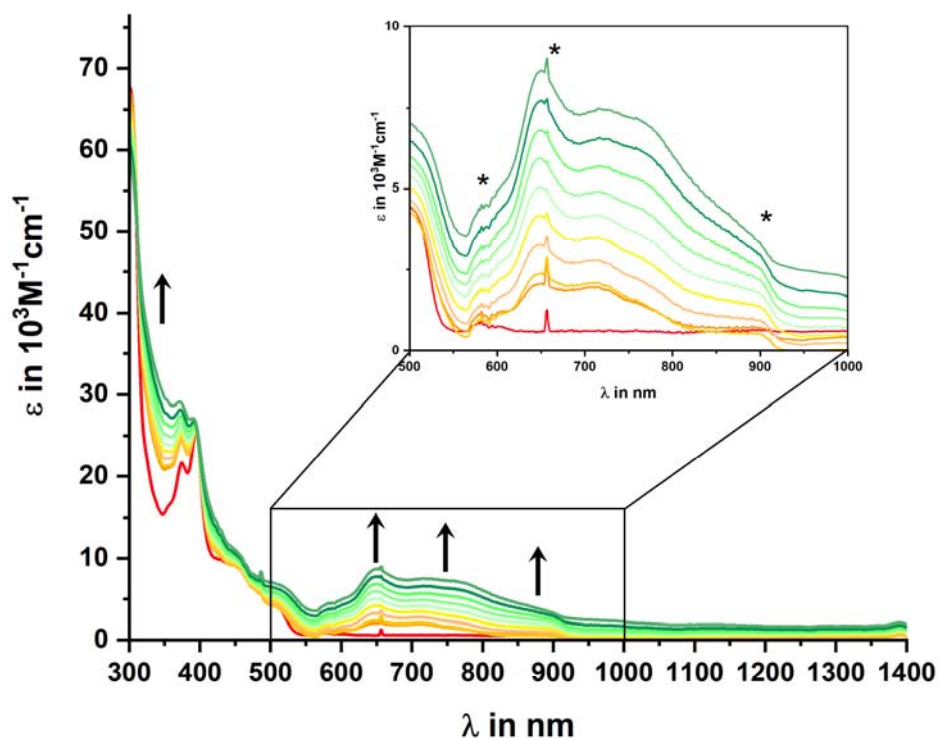


Figure 6. Changes of UV/vis/NIR spectra of $(\text{Idpc})_2$ (**9**) on reduction in 1,2-dichlorobenzene/ NBu_4PF_6 (0.1M); * Asterisks denote measurement artefacts of our setup during switching from UV to NIR (900nm) and during change from background measurement to sample (660, 580nm).

Conclusion

In summary, we prepared a series of indacenopicene–(ethynyl) arene derivatives by palladium catalyzed cross-coupling of **Idpc-Br** with differently substituted aryl boronates and ethynyl arenes. All products were characterized by UV/vis spectroscopy, luminescence spectroscopy and spectroelectrochemistry. Important intermediates were investigated by X-ray diffraction studies. The synthesized products represent the first members of a family where a functionalization of the rim-region of Idpc was achieved by C–C cross coupling reaction. All members are fluorescent in solution with quantum yields of up to 10%. The ethynyl bridged coupling products generally showed improved quantum yields over their aryl–aryl coupled counterparts. Both ferrocenyl derivatives Idpc-Fc (**8h**) and Idpc≡-Ph (**8i**) unexpectedly show fluorescence due to a strong decoupling of the organometallic moiety and the geodesic arene. This has been corroborated by quantum chemical calculations and above measurements. **Idpc-Br** is a superb cross-coupling partner and gives access to a whole family of aryl and phenylethynyl substituted indacenopicene derivatives in a single step in yields exceeding 80 %.

Experimental Section

UV/vis/NIR- and Luminescence Spectroscopy

UV/vis/NIR spectra on CH₂Cl₂ solutions of the respective compounds were recorded on a TIDAS fiber optic diode array spectrometer (combined MCS UV/NIR and PGS NIR instrumentation) from J&M in HELLMA quartz cuvettes with 0.1 cm optical path lengths. Luminescence spectra and lifetimes as well as quantum yields were measured in CH₂Cl₂ solutions on a PicoQuant FluoTime 300 spectrometer. Absolute quantum yields were determined with an integrating sphere within the PicoQuant FluoTime 300 spectrometer.

Cyclic Voltammetry

Cyclic voltammetry analysis was performed in a one-compartment cell with 5–7 mL of 1,2-dichlorobenzene as the solvent and NBu₄PF₆ (0.1 M) as the supporting electrolyte. A platinum electrode (Ø = 1.1 mm, BASI) was used as the working electrode. It was polished with diamond pastes (1.5 and 1 µm particle size) from Buehler and Wirtz before measurements. A computer-controlled BASi EPSILON potentiostat was used for recording the voltammograms. An Ag/AgCl wire pseudo reference electrode and a Pt-wire as auxiliary electrode were used in the measurements. The cell was connected to an argon-gas cylinder. Potential calibration was performed by adding appropriate quantities of decamethylferrocene (Cp*₂Fe) after all scans of interest had been acquired. Potentials are reported against the ferrocene/ferrocenium (Cp₂Fe^{0/+}) couple, which is 550 mV positive of the Cp*₂Fe^{0/+} couple under our conditions. Decamethylferrocene had to be used because of a too small

separation between the oxidation wave of ferrocene derivatives **8h** and **8l** and the usual ferrocene standard.

The OTTLE cell was also home-built and comprises of a Pt-mesh working and counter electrode and a thin silver wire as a pseudoreference electrode sandwiched between the CaF₂ windows of a conventional liquid IR cell. Its design follows that of Hartl et al.^[49] The working electrode is positioned in the center of the spectrometer beam. For every measurement, a Wenking POS 2 potentiostat by Bank Elektronik - Intelligent Controls GmbH was used. FT-IR spectra were recorded using a Bruker Tensor II FT-IR spectrometer. UV/Vis/NIR spectra were obtained on a TIDAS fiberoptic diode array spectrometer (combined MCS UV/NIR and PGS NIR instrumentation) from j&m Analytik AG.

Density Functional Theory (DFT) Calculations

The ground state electronic structures of the full models of the studied compounds were calculated by density functional theory (DFT) methods using the Gaussian 16 program packages.^[52] Geometry optimization followed by vibrational analysis was performed in solvent media. Solvent effects were described by the polarizable continuum model (PCM) with standard parameters for dichloromethane.^[53] For Fe, the ten-electron quasirelativistic effective core potential (ECP) MDF10 was used^[54] and 6-31G(d) polarized double- ζ basis sets^[55] for the remaining atoms were employed together with the Perdew, Burke, Ernzerhof exchange and correlation functional (PBE0).^[56-57] The GaussSum program package was used to analyze the results,^[58] while the visualization of the results was performed with the Avogadro program package.^[59] Graphical representations of molecular orbitals were generated with the help of GNU Parallel^[60] and plotted using the vmd program package^[61] in combination with POV-Ray.^[62]

General Methods

Dichloromethane and ethyl acetate for column chromatography were distilled prior to use. All experiments requiring inert atmosphere were carried out under nitrogen using Schlenk techniques. All other solvents and all commercially available reagents were used without any prior purification. ¹H, ¹³C and ¹⁹F NMR spectra were recorded on Bruker Avance NEO 800, Bruker Avance III 600, Bruker Avance III 400 and JEOL Resonance ECZ 400S. Deuterated solvents were purchased in sealed ampules and dried where necessary according to standard procedures.^[63] Structure assignments were done based on 2D-NMR (COSY, HSQC, HMBC, NOESY) experiments. ¹H-NMR chemical shifts are

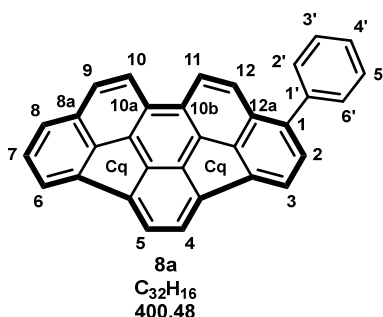
referenced with respect to the chemical shift of the residual protons present in the deuterated solvents ($C_2D_2Cl_4$ δ H = 5.91 ppm, δ C = 73.78 ppm; $CDCl_3$: δ H = 7.26 ppm, δ C = 77.16 ppm). EI-MS spectra were recorded on a JEOL JMS-Q1500GC with direct insertion probe; HR-EI-MS were recorded on a Waters Micromass GCT TOF spectrometer. IR spectra were recorded on a Perkin Elmer Spectrum 100 ATR unit using compounds in solid state. 4-Bromo-13,16-difluorobenzo[s]picene (**4**) was obtained by double photocyclization of the respective stilbenes according to the procedure described by Papaianina *et al.*^[23] Resulting 4-bromo-13,16-difluorobenzo[s]picene (**4**) and 4-bromo-13,16-difluorobenzo[s]picene (**4**) were purified by repeated precipitation from cold methanol. All stilbene derivatives were used as *cis/trans* isomeric mixtures as received from the Wittig reaction since the isomers do interconvert under photocyclization conditions. For the aluminum oxide promoted dehydrofluorination reaction, typically 3.0 g of γ - Al_2O_3 (neutral, EcoChrom, MP Biomedicals) were activated in Duran glassware at 525 °C for 30 min in vacuum (10^{-3} mbar). After cooling to 250 °C, fluoroarene (50 mg) was added and the reaction was carried out at 280 °C in vacuum (10^{-3} mbar) until full consumption of starting material was evident by EI-MS. After cooling to room temperature, products were transferred to a Soxhlet thimble and extracted using CH_2Cl_2 . Analytically pure products were obtained by precipitation with MeOH from the corresponding CH_2Cl_2 extract in typical yields of >90 %.

General procedure A (Suzuki coupling)

A Schlenk flask purged with nitrogen was charged with **Idpc-Br** (1 eq.), $Pd(PPh_3)_4$ (0.01 eq.), sodium carbonate (3 eq.), and the corresponding phenylboronic acid (1.5 eq) in a 1,4-dioxane/ H_2O solution. The reaction mixture was degassed by bubbling nitrogen via cannula through the mixture for 15 min. Then, the reaction mixture was heated under reflux conditions until full consumption of starting material was detected by TLC. The solvent was removed under reduced pressure and the residue was dissolved in CH_2Cl_2 (100 mL) and washed with saturated bicarbonate solution (100 mL) and brine (100 mL). The organic phase was dried over magnesium sulfate, filtered, and the residue was purified by silica gel chromatography using PE/ CH_2Cl_2 (3:1) as eluent.

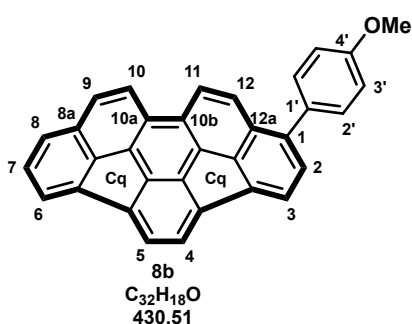
General procedure B (Sonogashira coupling)

A Schlenk flask purged with nitrogen was charged with **Br-Idpc** (1 eq.), CuI (0.025 eq.), $PdCl_2(PPh_3)_2$ (0.05 eq.), diisopropylamine (2 eq.), and the corresponding phenylacetylene (1.20 eq.). THF was added and the mixture was degassed by three freeze-pump-thaw cycles. Afterwards, the reaction mixture was heated to reflux until full consumption of starting material was detected by TLC. The volatiles were removed under reduced pressure and the residue was extracted with brine (100 mL) and CH_2Cl_2 (3 x 50 mL). The combined organic phases were dried over magnesium sulfate, filtered, and the residue was purified by silica gel chromatography using a mixture of toluene/ CH_2Cl_2 (5:2) as eluent.



Compound **8a** was synthesized according to general procedure A using **Idpc-Br** (80.0 mg, 0.20 mmol, 1.00 eq.), Pd(PPh₃)₄ (2.3 mg, 0.01 eq.), sodium carbonate (63.0 mg, 0.60 mmol, 3 eq.) and phenylboronic acid (36.3 mg, 1.5 eq) in a 1,4-dioxan/H₂O (14:1) solution (50 mL). Orange solid (67.0 mg, 0.17 mmol, 84%).

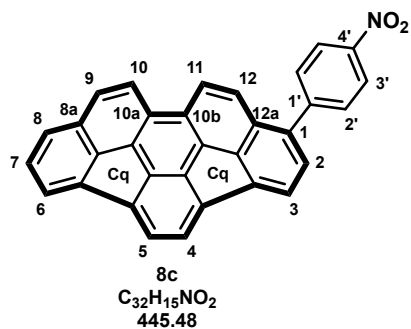
¹H NMR (600 MHz, C₂D₂Cl₄) δ = 8.05 (d, ³J_{HH} = 8.8 Hz, 1H, *H10*), 8.04 (d, ³J_{HH} = 8.9 Hz, 1H, *H11*), 7.86 (d, ³J_{HH} = 8.9 Hz, 1H, *H12*), 7.74 (d, ³J_{HH} = 8.7 Hz, 1H, *H9*), 7.73 (d, ³J_{HH} = 7.2 Hz, 1H, *H3*), 7.67 (d, ³J_{HH} = 6.9 Hz, 1H, *H6*), 7.64 (bs, 2H, *H4* + *H5*), 7.63 – 7.58 (m, 3H, *H8* + *H2'* + *H6'*), 7.50 – 7.45 (m, 2H, *H3'* + *H5'*), 7.43 – 7.40 (m, 1H, *H4'*), 7.38 (d, ³J_{HH} = 7.2 Hz, 1H, *H2*) 7.36 (dd, ³J_{HH} = 8.2, 7.0 Hz, 1H, *H7*); ¹³C NMR (150 MHz, C₂D₂Cl₄) δ = 140.59 (*CI*), 138.85 (*CI'*), 138.71 (*Cq*), 138.54 (*Cq*), 138.17 (*Cq*), 138.14 (*Cq*), 138.02 (*Cq*), 138.00 (2C, *Cq*), 137.77 (*Cq*), 137.05 (*Cq*), 136.42 (*Cq*), 129.74 (*CI0b*), 129.69 (*CI0a*), 129.68 (2C, *C2'* + *C6'*), 129.00 (*C2*), 128.94 (*C8a*), 128.88 (*C7*), 128.55 (2C, *C3'* + *C5'*), 127.69 (*C4'*), 127.12 (*CI2a*), 126.93 (*C9*), 126.74 (*C8*), 126.17 (*CI2*), 125.67 (*C5*), 125.43 (*C4*), 124.19 (*CI0*), 123.94 (*CI1*), 123.82 (*C3*), 123.58 (*C6*); IR (cm⁻¹) 2891, 1856, 1547, 1480, 1392, 1254, 1137, 1100, 1071, 1011, 940, 799, 781, 752, 704; MS (EI): *m/z* (rel. int.) = 400 (100%), 323 (40 %); HRMS (EI) *m/z* Calcd for C₃₂H₁₆ [M]⁺: 400.1252. Found: 400.1256.



Compound **8b** was synthesized according to general procedure A using **Idpc-Br** (80.0 mg, 0.20 mmol, 1.00 eq.), Pd(PPh₃)₄ (2.30 mg, 0.01 eq.), sodium carbonate (63.0 mg, 0.60 mmol, 3.00 eq.) and 4-methoxyphenylboronic acid (45.2 mg, 1.50 eq.) in a 1,4-dioxan/H₂O (14:1) solution (50 mL). Orange solid (67.5 mg, 0.16 mmol, 79 %).

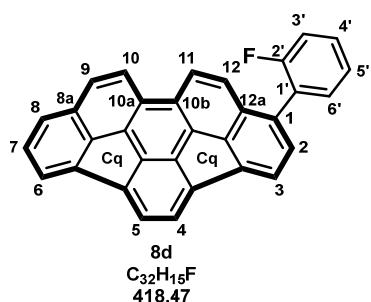
¹H NMR (600 MHz, C₂D₂Cl₄) δ = 8.03 (d, ³J_{HH} = 8.7 Hz, 1H, *H10*), 8.02 (d, ³J_{HH} = 9.0 Hz, 1H, *H11*), 7.86 (d, ³J_{HH} = 8.8 Hz, 1H, *H12*), 7.72 (d, ³J_{HH} = 8.7 Hz, 1H, *H9*), 7.70 (d, ³J_{HH} = 7.2 Hz, 1H, *H3*), 7.65 (d, ³J_{HH} = 6.9 Hz, 1H, *H6*), 7.61 (s, 2H, *H4* + *H5*), 7.58 (d, ³J_{HH} = 8.1 Hz, 1H, *H8*), 7.55 (d, ³J_{HH} = 8.6 Hz, 2H, *H2'*), 7.34 (dd, ³J_{HH} = 8.0, 7.0 Hz, 2H, *H2* + *H7*), 7.02 (d, ³J_{HH} = 8.6 Hz, 2H, *H3'*), 3.84 (s, 3H, *OMe*); ¹³C NMR (150 MHz, C₂D₂Cl₄) δ = 159.15 (*C4'*), 140.26 (*CI*), 138.71 (*Cq*), 138.37 (*Cq*), 138.16 (*Cq*), 138.08 (*Cq*), 137.99 (*Cq*), 137.91 (*Cq*), 137.70 (*Cq*), 137.53 (*Cq*), 137.10 (*Cq*), 136.38 (*Cq*), 131.34 (*CI'*), 130.81 (2C, *C2'*), 129.66 (*CI0b*), 129.64 (*CI0a*), 128.90 (*C8a*), 128.83 (*C7*), 128.59 (*C2*), 127.19 (*CI2a*), 126.86 (*C9*), 126.67 (*C8*), 126.24

(*C12*), 125.62 (*C5*), 125.27 (*C4*), 124.06 (*C11*), 123.91 (*C10*), 123.87 (*C3*), 123.50 (*C6*), 114.01 (2*C*, *C3'*), 55.39 (*OMe*); $^1\text{H NMR}$ (400 MHz, CDCl_3) δ = 8.09 (dd, J = 8.5 Hz, 2H, *H10* + *H11*), 7.91 (d, J = 8.8 Hz, 1H, *H12*), 7.77 (d, J = 8.7 Hz, 1H, *H9*), 7.74 (d, J = 7.1 Hz, 1H, *H3*), 7.71 (d, J = 6.9 Hz, 1H, *H6*), 7.67 (s, 2H, *H4* + *H5*), 7.64 (d, J = 8.1 Hz, 1H, *H8*), 7.61 (d, J = 8.6 Hz, 2H, *H2'*), 7.40 (dd, J = 8.0, 6.9 Hz, 1H, *H7*), 7.38 (d, J = 7.0 Hz, 1H, *H2*), 7.08 (d, J = 8.6 Hz, 2H, *H3'*), 3.91 (s, 3H, *OMe*); $^{13}\text{C NMR}$ (100 MHz, CDCl_3) δ = 159.56 (*C4'*), 140.57 (*C1*), 139.18 (*Cq*), 138.76 (*Cq*), 138.61 (*Cq*), 138.56 (*Cq*), 138.49 (*Cq*), 138.40 (*Cq*), 138.16 (*Cq*), 138.00 (*Cq*), 137.58 (*Cq*), 136.87 (*Cq*), 131.83 (*C1'*), 131.03 (2*C*, *C2'*), 130.07 (*C10b*), 130.04 (*C10a*), 129.24 (*C8a*), 128.90 (*C7*), 128.68 (*C2*), 127.59 (*C12a*), 126.96 (*C9*), 126.78 (*C8*), 126.40 (*C12*), 125.69 (*C5*), 125.34 (*C4*), 124.28 (*C11*), 124.12 (*C10*), 123.81 (*C3*), 123.48 (*C6*), 114.20 (2*C*, *C3'*), 55.56 (*OMe*); **IR** (cm^{-1}) 2981, 1856, 1607, 1515, 1480, 1247, 1178, 1101, 951, 809; **MS** (EI): m/z (*rel. int.*) = 430 (100 %), 399 (50 %), 323 (30 %).



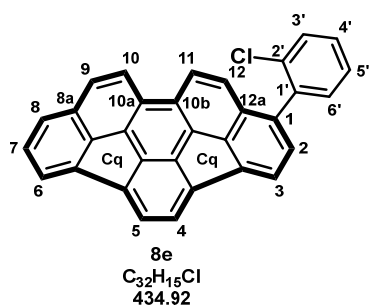
Compound **8c** was synthesized according to general procedure A using **Idpc-Br** (80.0 mg, 0.20 mmol, 1.00 eq.), $\text{Pd}(\text{PPh}_3)_4$ (2.3 mg, 0.01 eq.), sodium carbonate (63.0 mg, 0.60 mmol, 3 eq.) and 4-nitrophenylboronic acid (49.7 mg, 1.5 eq.) in a 1,4-dioxan/ H_2O (2:1) solution (50 mL). Red solid (73.3 mg, 0.16 mmol, 83 %).

$^1\text{H NMR}$ (600 MHz, $\text{C}_2\text{D}_2\text{Cl}_4$) δ = 8.31 (d, $^3J_{\text{HH}}$ = 8.2 Hz, 2H, *H3'*), 8.09 – 8.02 (m, 2H, *H10* + *H11*), 7.76 - 7.71 (m, 5H, *H3* + *H9* + *H12* + *H2'*), 7.68 (d, $^3J_{\text{HH}}$ = 6.9 Hz, 1H, *H6*), 7.65 (s, 2H), 7.61 (d, $^3J_{\text{HH}}$ = 8.0 Hz, 1H, *H8*), 7.38 (d, $^3J_{\text{HH}}$ = 7.1 Hz, 1H, *H2*), 7.37 (dd, $^3J_{\text{HH}}$ = 7.9, 6.9 Hz, 1H, *H7*); $^{13}\text{C NMR}$ (150 MHz, $\text{C}_2\text{D}_2\text{Cl}_4$) δ = 146.98 (*C4'*), 145.80 (*C1'*), 139.44 (*C1*), 138.97 (*Cq*), 138.58 (*Cq*), 138.17 (*Cq*), 138.03 (*Cq*), 137.86 (*Cq*), 137.76 (*Cq*), 137.72 (*Cq*), 137.02 (*Cq*), 136.38 (*Cq*), 130.41 (2*C*, *C3'*), 129.97 (*C10b*), 129.54 (*C2*), 129.02 (*C7*), 129.00 (*C10a*), 128.19 (*C8a*), 127.08 (*C3*), 126.91 (*C8*), 126.49 (*C12a*), 125.84 (2*C*, *C4* + *C5*), 125.11 (*C10*), 124.96 (*C9*), 123.91 (*C12*), 123.82 (2*C*, *C2'*), 123.77 (*C11*), 123.57 (*C6*); **IR** (cm^{-1}) 3035, 1922, 1730, 1593, 1509, 1421, 1341, 1107, 1012, 953, 861, 837, 823, 801, 782, 753, 702; **MS** (EI): m/z (*rel. int.*) = 445 (100 %), 399 (30 %), 323 (60 %).



Compound **8d** was synthesized according to general procedure A using **Idpc-Br** (80.0 mg, 0.20 mmol, 1.00 eq.), Pd(PPh₃)₄ (2.30 mg, 0.01 eq.), sodium carbonate (63.0 mg, 0.60 mmol, 3.00 eq.) and 2-fluorophenylboronic acid (41.6 mg, 1.50 eq.) in a 1,4-dioxan/H₂O (14:1) solution (50 mL). orange solid (74.5 mg, 0.18 mmol, 89%).

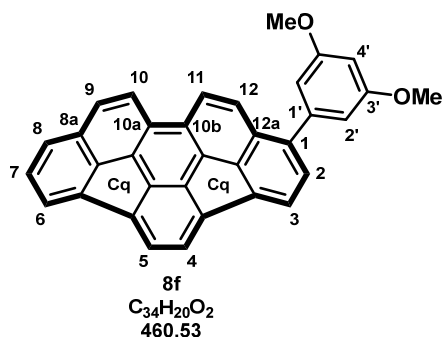
¹H NMR (600 MHz, C₂D₂Cl₄) δ = 8.01 (d, ³J_{HH} = 8.7 Hz, 1H, *H10*), 8.00 (d, ³J_{HH} = 8.9 Hz, 1H, *H11*), 7.73 – 7.70 (m, 2H, *H3* + *H9*), 7.65 (d, ³J_{HH} = 6.9 Hz, 1H, *H6*), 7.62 (dd, ³J_{HH} = 8.9, 2.2 Hz, 1H, *H12*), 7.60 (bs, 2H, *H4* + *H5*), 7.58 (d, ³J_{HH} = 8.1 Hz, 1H, *H8*), 7.46 (dd, ³J_{HH} = 7.5, 1.7 Hz, 1H, *H6'*), 7.41 (ddd, *J* = 9.9, 4.9, 2.3 Hz, 1H, *H4'*), 7.37 (d, ³J_{HH} = 7.1 Hz, 1H, *H2*), 7.34 (dd, ³J_{HH} = 8.1, 7.0 Hz, 1H, *H7*), 7.25 (m, 1H, *H5'*), 7.21 (m, 1H, *H3'*); ¹⁹F NMR (375 MHz, C₂D₂Cl₄) δ = -113.88; ¹³C NMR (150 MHz, C₂D₂Cl₄) δ = 159.61 (d, *J* = 247.5 Hz, *C2'*), 138.70 (*Cq*), 138.62 (*Cq*), 138.61 (*Cq*), 138.13 (*Cq*), 138.09 (*Cq*), 138.01 (*Cq*), 137.94 (*Cq*), 137.76 (*Cq*), 136.66 (*Cq*), 136.39 (*Cq*), 134.08 (*CI*), 132.17 (d, *J* = 3.3 Hz, *C6'*), 130.18 (*C2*), 129.79 (*CI0b*), 129.74 (*C7*), 129.62 (*CI0a*), 128.87 (d, *J* = 6.8 Hz, *C4'*), 128.85 (*C8a*), 127.60 (*CI2a*), 126.90 (*C9*), 126.75 (*C8*), 126.27 (d, *J* = 15.3 Hz, *CI'*), 125.99 (d, *J* = 2.3 Hz, *CI2*), 125.64 (*C5*), 125.57 (*C4*), 124.29 (d, *J* = 3.5 Hz, *C5'*), 124.16 (*CI1*), 123.88 (*CI0*), 123.59 (*C6*), 123.49 (*C3*), 115.93 (d, *J* = 22.2 Hz, *C3'*); IR (cm⁻¹) 2957, 2874, 1464, 1381, 1251, 1129, 1097, 1073, 1004, 943, 793, 779, 753, 739; MS (EI): *m/z* (rel. int.) = 418 (100%), 399 (80%), 323 (30%).



Compound **8e** was synthesized according to general procedure A using **Idpc-Br** (80.0 mg, 0.20 mmol, 1.00 eq.), Pd(PPh₃)₄ (2.30 mg, 0.01 eq.), sodium carbonate (63.0 mg, 0.60 mmol, 3.00 eq.) and 2-chlorophenylboronic acid (46.5 mg, 1.50 eq.) in a 1,4-dioxan/H₂O (14:1) solution (50 mL). Orange solid (75.0 mg, 0.17 mmol, 87%).

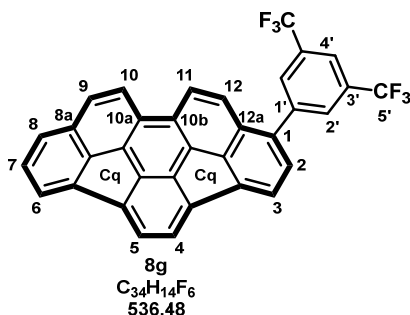
¹H NMR (600 MHz, CDCl₃) δ = 8.11 (d, ³J_{HH} = 8.7 Hz, 1H, *H10*), 8.07 (d, ³J_{HH} = 8.8 Hz, 1H, *H11*), 7.79 (d, ³J_{HH} = 8.7 Hz, 1H, *H9*), 7.78 (d, ³J_{HH} = 7.1 Hz, 1H, *H3*), 7.73 (d, ³J_{HH} = 6.9 Hz, 1H, *H6*), 7.72 – 7.68 (m, 2H, *H4* + *H5*), 7.65 (d, ³J_{HH} = 8.0 Hz, 1H, *H8*), 7.59 – 7.56 (m, 1H, *H3'*), 7.53 (d, ³J_{HH} = 8.8 Hz, 1H, *H12*), 7.45 – 7.43 (m, 1H, *H6'*), 7.43 – 7.38 (m, 3H, *H7* + *H4'* + *H5'*), 7.34 (d, ³J_{HH} = 7.1 Hz, 1H, *H2*); ¹³C NMR (150 MHz, CDCl₃) δ = 139.17 (*Cq*), 139.07 (*Cq*), 139.00 (*Cq*), 138.80 (*Cq*), 138.68 (*Cq*), 138.67 (*Cq*), 138.60 (*Cq*), 138.37 (*Cq*), 138.03 (*CI'*), 137.91 (*CI*), 137.00 (*Cq*), 136.93 (*Cq*), 133.83 (*C2'*), 132.30 (*C6'*), 130.24 (*CI0b*), 130.15 (*CI0a*), 130.03 (*C2*), 129.99 (*C3'*), 129.33 (*C4'*), 129.26 (*C8a*), 128.94 (*C7*), 128.01 (*CI2a*), 127.06 (*C9*),

126.88 (C8), 126.80 (C5'), 126.17 (C12), 125.75 (C5), 125.73 (C4), 124.32 (C11), 124.15 (C10), 123.58 (C6), 123.30 (C3); IR (cm⁻¹) 2923, 2360, 1511, 1412, 1241, 1134, 1015, 960, 821, 808, 756; MS (EI): *m/z* (rel. int.) = 434 (100 %), 399 (50 %), 323 (30 %).



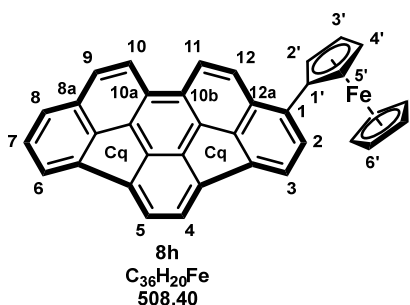
Compound **8f** was synthesized according to general procedure A using **Idpc-Br** (80.0 mg, 0.20 mmol, 1.00 eq.), Pd(PPh₃)₄ (2.3 mg, 0.01 eq.), sodium carbonate (63.0 mg, 0.60 mmol, 3 eq.) and 3,5-dimethoxyphenylboronic acid (54.1 mg, 1.5 eq.) in a 1,4-dioxan/H₂O (14:1) solution (50 mL). Orange solid (69.4 mg, 0.16 mmol, 76 %).

¹H NMR (600 MHz, C₂D₂Cl₄) δ = 8.03 (d, ³J_{HH} = 8.8 Hz, 1H, *H11*), 8.03 (d, ³J_{HH} = 8.8 Hz, 1H, *H10*) 7.91 (d, ³J_{HH} = 8.9 Hz, 1H, *H12*), 7.72 (d, ³J_{HH} = 8.7 Hz, 1H, *H9*), 7.71 (d, ³J_{HH} = 7.3 Hz, 1H, *H3*), 7.66 (d, ³J_{HH} = 6.9 Hz, 1H, *H6*), 7.62 (s, 2H, *H4* + *H5*), 7.59 (d, ³J_{HH} = 8.1 Hz, 1H, *H8*), 7.38 (d, ³J_{HH} = 7.2 Hz, 1H, *H2*), 7.34 (dd, ³J_{HH} = 8.2, 7.0 Hz, 1H, *H7*), 6.75 (d, ⁴J_{HH} = 2.3 Hz, 2H, *H2'*), 6.52 (t, ⁴J_{HH} = 2.3 Hz, 1H, *H4'*). 3.81 (s, 6H, **2x OMe**); ¹³C NMR (150 MHz, C₂D₂Cl₄) δ = 160.53 (2C, *C3'*), 140.95 (*C1'*), 140.38 (*C1*), 138.67 (*Cq*), 138.54 (*Cq*), 138.16 (*Cq*), 138.10 (2C, *Cq*), 137.97 (2C, *Cq*), 137.73 (*Cq*), 136.99 (*Cq*), 136.39 (*Cq*), 129.74 (*C10b*), 129.62 (*C10a*), 128.91 (*C8a*), 128.86 (*C2*), 128.79 (*C7*), 127.03 (*C12a*), 126.90 (*C9*), 126.73 (*C8*), 126.13 (*C12*), 125.64 (*C5*), 125.43 (*C4*), 124.20 (*C11*), 123.91 (*C10*), 123.69 (*C3*), 123.56 (*C6*), 107.91 (*C2'*), 99.64 (*C4'*), 55.50 (2C, **2x OMe**); ¹H NMR (400 MHz, CDCl₃) δ = 8.07 (d, *J* = 8.8 Hz, 2H, *H10* + *H11*), 7.94 (d, *J* = 8.9 Hz, 1H, *H12*), 7.75 (d, *J* = 8.7 Hz, 1H, *H9*), 7.73 (d, *J* = 7.1 Hz, 1H, *H3*), 7.69 (d, *J* = 6.9 Hz, 1H, *H6*), 7.64 (s, 2H, *H4* + *H5*), 7.62 (d, *J* = 8.1 Hz, 1H, *H8*), 7.42 (d, *J* = 7.1 Hz, 1H, *H2*), 7.38 (dd, *J* = 8.1, 6.9 Hz, 1H, *H7*), 6.81 (d, *J* = 2.3 Hz, 2H, *H2'*), 6.58 (t, *J* = 2.3 Hz, 1H, *H4'*), 3.89 (s, 6H, **2x OMe**); ¹³C NMR (100 MHz, CDCl₃) δ = 160.94 (2C, *C3'*), 141.39 (*C1'*), 140.70 (*C1*), 139.12 (*Cq*), 138.87 (*Cq*), 138.58 (*Cq*), 138.51 (*Cq*), 138.47 (*Cq*), 138.40 (*Cq*), 138.38 (*Cq*), 138.12 (*Cq*), 137.44 (*Cq*), 136.83 (*Cq*), 130.09 (*C10b*), 129.97 (*C10a*), 129.22 (*C8a*), 128.88 (*C2*), 128.83 (*C7*), 127.39 (*C12a*), 126.95 (*C9*), 126.80 (*C8*), 126.26 (*C12*), 125.67 (*C5*), 125.45 (*C4*), 124.40 (*C11*), 124.09 (*C10*), 123.61 (*C3*), 123.50 (*C6*), 108.13 (*C2'*), 99.86 (*C4'*), 55.66 (2C, **2x OMe**); IR (cm⁻¹) 2956, 1592, 1455, 1421, 1264, 1204, 1155, 1066, 896, 810, 728; MS (EI): *m/z* (rel. int.) = 460 (100 %) 323 (40 %).



Compound **8g** was synthesized according to general procedure A using **Idpc-Br** (80.0 mg, 0.20 mmol, 1.00 eq.), Pd(PPh₃)₄ (2.30 mg, 0.01 eq.), sodium carbonate (63.0 mg, 0.60 mmol, 3.00 eq.) and 3,5-methoxyphenylboronic acid (76.7 mg, 1.50 eq.) in a 1,4-dioxan/H₂O (14:1) solution (50 mL). Orange solid (67.5 mg, 0.16 mmol, 79 %).

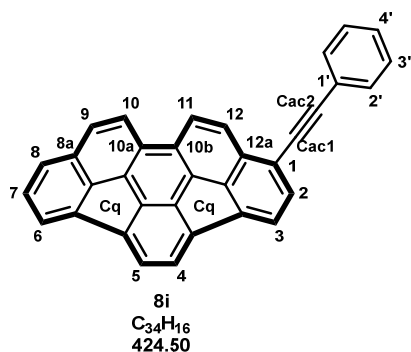
¹H NMR (400 MHz, CDCl₃) δ = 8.12 – 8.09 (m, 3H, *H11* + *H2'*), 8.07 (d, *J* = 8.7 Hz, 1H, *H10*), 7.98 (bs, 1H, *H4'*), 7.78 (d, *J* = 8.7 Hz, 1H, *H9*), 7.75 (d, *J* = 7.1 Hz, 1H, *H3*), 7.72 (d, *J* = 6.9 Hz, 1H, *H6*), 7.69 (d, *J* = 8.8 Hz, 1H, *H12*), 7.66 (s, 2H, *H4* + *H5*), 7.65 (d, *J* = 8.1 Hz, 1H, *H8*), 7.41 (dd, *J* = 8.1, 6.9 Hz, 1H, *H7*), 7.40 (d, *J* = 7.1 Hz, 1H, *H2*); ¹⁹F NMR (375 MHz, C₂D₂Cl₄) δ = -62.22; ¹³C NMR (100 MHz, CDCl₃) δ = 141.48 (*CI'*), 139.96 (*Cq*), 139.36 (*Cq*), 139.04 (*Cq*), 138.58 (*Cq*), 138.43 (*Cq*), 138.32 (*Cq*), 138.24 (*Cq*), 138.02 (*Cq*), 137.47 (*Cq*), 137.11 (*Cq*), 136.82 (*CI*), 132.13 (q, ²*J*_{CF} = 33.3 Hz, (2C, *C3'*), 130.31 (*CI0b*), 129.82(*CI0a*), 129.80 (m, 2C, *C2'*), 129,60 (*C2*), 129.34(*C8a*), 129.08 (*C7*), 127.16 (*C9*), 127.02 (*C8*), 126.69 (*CI2a*), 125.89 (*C5*), 125.88 (*C4*), 125.37 (*CI1*), 124.71 (*CI2*), 124.07 (*CI0*), 123.75 (*C6*), 123.47 (*C3*), 123.51 (q, ¹*J*_{CF} = 272.9 Hz, *C5'*) 121.51-121.49 (hept, ³*J*_{CF} = 3.6 Hz, *C4'*); IR (cm⁻¹) 2957, 2875, 1464, 1421, 1382, 1215, 1149, 1065, 892, 807, 731; MS (EI): *m/z* (rel. int.) = 536 (100 %) 467 (30 %) 398 (20 %), 323 (50 %).



Compound **8h** was synthesized according to general procedure A using **Idpc-Br** (80.0 mg, 0.20 mmol, 1.00 eq.), Pd(PPh₃)₄ (2.3 mg, 0.01 eq.), sodium carbonate (63.0 mg, 0.60 mmol, 3 eq.) and ferroceneboronic acid (68.4 mg, 1.5 eq) in a 1,4-dioxane/H₂O (14:1) solution (50 mL). Red solid (84.7 mg, 0.17 mmol, 84 %). Crystals suitable for X-ray diffraction were grown by slow diffusion of *n*-hexane into a concentrated solution of **8h** in CH₂Cl₂.

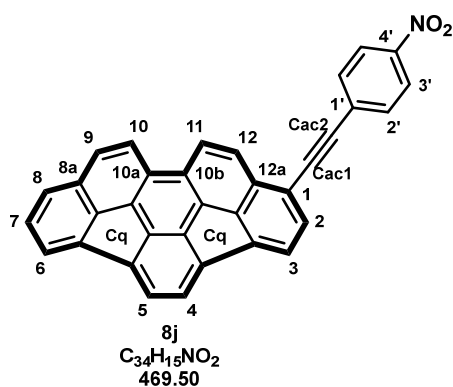
¹H NMR (600 MHz, C₂D₂Cl₄): δ = 8.38 (d, ³*J*_{HH} = 8.9 Hz, 1H, *H12*), 8.13 (d, ³*J*_{HH} = 8.9 Hz, 1H, *H11*), 8.11 (d, ³*J*_{HH} = 8.8 Hz, 1H, *H10*), 7.78 (d, ³*J*_{HH} = 8.7 Hz, 1H, *H9*), 7.69 (d, ³*J*_{HH} = 6.9 Hz, 1H, *H6*), 7.65 (d, ³*J*_{HH} = 7.4 Hz, 1H, *H5*), 7.62j (d, ³*J*_{HH} = 7.7 Hz, 2H, *H8* + *H4*), 7.59 (d, ³*J*_{HH} = 7.3 Hz, 1H, *H3*), 7.48 (d, ³*J*_{HH} = 7.4 Hz, 1H, *H2*), 7.37 (t, ³*J*_{HH} = 7.5 Hz, 1H, *H7*), 4.82 (s, 2H, *H2'*), 4.46 (s, 2H, *H3'*), 4.13 (s, 5H, *H4'*); ¹³C NMR (150 MHz, C₂D₂Cl₄) δ = 138.80 (*Cq*), 138.45 (*Cq*), 138.29 (*Cq*), 138.21 (*Cq*), 138.09 (*Cq*), 138.07 (*Cq*), 137.81 (*Cq*), 137.61 (*Cq*), 137.08 (*CI*), 136.87 (*Cq*), 136.44

(*Cq*), 129.61 (*CI0a*), 129.50 (*CI0b*), 128.96 (*C8a*), 128.90 (*C7*), 128.34 (*C2*), 127.33 (*CI2a*), 126.93 (*C9*), 126.68 (*C8*), 126.41 (*CI2*), 125.67 (*C5*), 125.07 (*C4*), 123.99 (*CI0*), 123.61 (*C3*), 123.55 (*C6*), 123.50 (*CI1*), 74.04 (*CI'*), 70.33 (5*C*, *C4'*), 69.73 (2*C*, *C2'*), 69.64 (2*C*, *C3'*); **IR** (cm⁻¹) 2958, 2875, 1463, 1382, 1251, 1151, 1073, 956, 817, 740; **MS** (EI): *m/z* (*rel. int.*) = 508 (100 %), 323 (60 %); **HRMS** (EI) *m/z* Calcd for C₃₆H₂₀Fe [M]⁺: 508.0914. Found: 508.0916.



Compound **8i** was synthesized according to general procedure B using **Idpc-Br** (0.1 g, 0.24 mmol, 1.00 eq.), CuI (1.2 mg, 0.025 eq.), PdCl₂(PPh₃)₂ (8.4 mg, 0.05 eq.), diisopropylamine (0.1 mL, 2.00 eq.) and phenylacetylene (0.04 mL, 0.29 mmol, 1.20 eq.) dissolved in 20 ml THF. Red solid (90.4 mg, 0.21 mmol, 89 %).

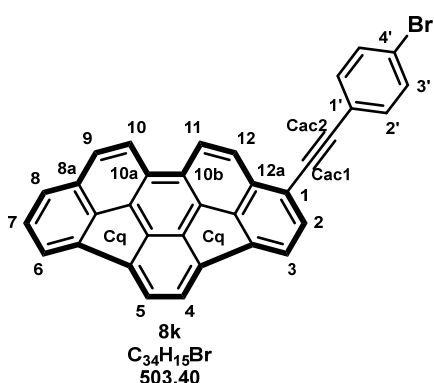
¹H NMR (600 MHz, C₂D₂Cl₄) δ = 8.12 (d, *J* = 8.8 Hz, 1H, *H11*), 8.07 (d, *J* = 8.7 Hz, 1H, *H10*), 8.05 (d, *J* = 8.7 Hz, 1H, *H12*), 7.77 (d, *J* = 8.7 Hz, 1H, *H9*), 7.68 (d, *J* = 6.9 Hz, 1H, *H6*), 7.64 (d, *J* = 7.2 Hz, 1H, *H3*), 7.63 – 7.60 (m, 4H, *H4* + *H5* + *H3'*), 7.57 (d, *J* = 7.2 Hz, 1H, *H2*), 7.39 – 7.32 (m, 4H, *H7* + *H8*, *H2'*), 7.28 – 7.22 (m, 1H, *H4'*); ¹³C NMR (150 MHz, C₂D₂Cl₄) δ = 138.89 (*Cq*), 138.71 (*Cq*), 138.57 (*Cq*), 138.19 (*Cq*), 138.07 (*Cq*), 138.05 (*Cq*), 138.01 (*Cq*), 137.84 (*Cq*), 136.44 (*Cq*), 136.33 (*Cq*), 132.83 (*C2*), 131.73 (2*C*, *C2'*), 130.23 (*CI0b*), 129.73 (*CI0a*), 129.06 (*CI2a*), 128.99 (*C7*), 128.98 (*C8a*), 128.70 (*C4'*), 128.47 (2*C*, *C3'*), 127.07 (*C9*), 126.89 (*C8*), 125.85 (*C5*), 125.77 (*C4*), 125.55 (*CI2*), 124.55 (*CI1*), 123.97 (*CI0*), 123.75 (*C6*), 123.34 (*C3*), 122.82 (*CI'*), 120.72 (*CI*), 95.31 (*Cac2*), 87.05 (*Cac1*); **IR** (cm⁻¹) 2957, 2873, 1463, 1380, 1209, 1138, 1067, 955, 836, 812, 741; **MS** (EI): *m/z* (*rel. int.*) = 424 (100 %), 323 (40 %).



Compound **8j** was synthesized according to general procedure B using **Idpc-Br** (0.1 g, 0.24 mmol, 1.00 eq.), CuI (1.2 mg, 0.025 eq.), PdCl₂(PPh₃)₂ (8.4 mg, 0.05 eq.), diisopropylamine (0.1 mL, 2.00 eq.) and 4-nitrophenylacetylene (43.0 mg, 0.29 mmol, 1.20 eq.) dissolved in 20 ml THF. Red solid (93.5 mg, 0.20 mmol, 83 %).

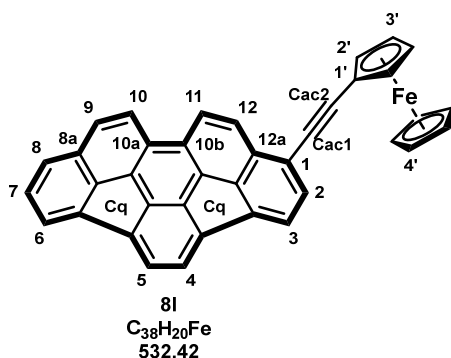
¹H NMR (600 MHz, C₂D₂Cl₄) δ = 8.19 (d, *J* = 8.7 Hz, 2H, *H3'*), 8.13 (d, *J* = 8.8 Hz, 1H, *H11*), 8.07 (d, *J* = 8.7 Hz, 1H, *H10*), 8.00 (d, *J* = 8.7 Hz, 1H, *H12*), 7.77 (d, *J* = 8.7 Hz, 1H, *H9*), 7.73 (d, *J* = 8.8 Hz, 2H, *H2'*), 7.69 (d, *J* = 6.9 Hz, 1H, *H6*), 7.66 (d, *J* = 7.2 Hz, 1H, *H3*), 7.64 – 7.59 (m, 4H, *H2* + *H4* + *H5* + *H8*), 7.46

(dd, $J = 8.1, 6.9$ Hz, 1H, *H7*); ^{13}C NMR (150 MHz, $\text{C}_2\text{D}_2\text{Cl}_4$) $\delta = 146.81$ (*C4'*), 139.75 (*Cq*), 139.20 (*Cq*), 138.50 (*Cq*), 138.22 (*Cq*), 138.10 (*Cq*), 138.02 (*Cq*), 137.89 (*Cq*), 137.83 (*Cq*), 136.44 (*Cq*), 136.33 (*Cq*), 133.69 (*C2*), 132.41 (*2C, C2'*), 130.36 (*C10b*), 129.99 (*C1'*), 129.66 (*C10a*), 129.06 (*C7*), 129.03 (*C8a*), 128.90 (*C12a*), 127.16 (*C9*), 127.00 (*C8*), 126.11 (*C5*), 125.85 (*C4*), 125.22 (*C12*), 124.92 (*C11*), 123.94 (*C10*), 123.86 (*C6*), 123.65 (*2C, C3'*), 123.20 (*C3*), 119.34 (*C1*), 93.13 (*Cac2*), 92.44 (*Cac1*); IR (cm^{-1}): 3046, 1902, 1859, 1547, 1480, 1421, 1392, 1253, 1136, 1099, 1071, 1010, 940, 890, 857, 816, 798, 778, 751, 704; MS (EI): m/z (*rel. int.*) = 469 (100 %), 323 (30 %); Anal. Calcd for $\text{C}_{34}\text{H}_{15}\text{NO}_2$: 86.98 % (C), 3.22 % (H), 2.98 % (N), Found: 86.69 % (C), 3.55 % (H), 3.09 % (N).



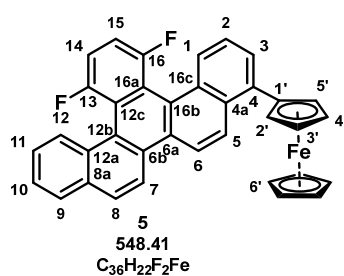
Compound **8k** was synthesized according to general procedure B using **Idpc-Br** (0.1 g, 0.24 mmol, 1.00 eq.), CuI (1.2 mg, 0.025 eq.), $\text{PdCl}_2(\text{PPh}_3)_2$ (8.4 mg, 0.05 eq.), diisopropylamine (0.1 mL, 2.00 eq.) and 4-bromophenylacetylene (53.0 mg, 0.29 mmol, 1.20 eq.) dissolved in 20 ml THF. Red solid (102 mg, 0.20 mmol, 82 %).

^1H NMR (600 MHz, $\text{C}_2\text{D}_2\text{Cl}_4$) $\delta = 8.10$ (d, $J = 8.8$ Hz, 1H, *H11*), 8.06 (d, $J = 8.6$ Hz, 1H, *H10*), 8.00 (d, $J = 8.7$ Hz, 1H, *H12*), 7.76 (d, $J = 8.7$ Hz, 1H, *H9*), 7.68 (d, $J = 6.8$ Hz, 1H, *H6*), 7.64 – 7.58 (m, 4H, *H3 + H4 + H5 + H8*), 7.56 (d, $J = 7.2$ Hz, 1H, *H2*), 7.52 – 7.44 (m, 4H, *H2' + H3'*), 7.37 (t, $J = 7.5$ Hz, 1H, *H7*); ^{13}C NMR (150 MHz, $\text{C}_2\text{D}_2\text{Cl}_4$) $\delta = 138.94$ (*2C, Cq*), 138.56 (*Cq*), 138.18 (*Cq*), 138.05 (*Cq*), 137.98 (*2C, Cq*), 137.83 (*Cq*), 136.43 (*Cq*), 136.32 (*Cq*), 133.13 (*2C, C2'*), 132.96 (*C2*), 131.67 (*2C, C3'*), 130.24 (*C10b*), 129.68 (*C10a*), 129.00 (*C7*), 128.99 (*8a*), 128.95 (*12a*), 127.07 (*C9*), 126.91 (*C8*), 125.88 (*C5*), 125.77 (*C4*), 125.42 (*C12*), 124.61 (*C11*), 123.94 (*C10*), 123.76 (*C6*), 123.29 (*C3*), 122.78 (*1'*), 121.89 (*4'*), 120.31 (*C1*), 94.14 (*Cac2*), 88.20 (*Cac1*); IR (cm^{-1}) 3046, 2210, 1871, 1859, 1547, 1480, 1421, 1392, 1253, 1137, 1099, 1071, 1010, 940, 890, 857, 816, 798, 778, 751, 704; MS (EI): m/z (*rel. int.*) = 504 (95 %), 502 (100 %), 423 (40 %), 323 (30 %).



Compound **8I** was synthesized according to general procedure B using aryl **Idpc-Br** (83.0 mg, 0.21 mmol, 1.00 eq.), CuI (1.0 mg, 0.025 eq.), PdCl₂(PPh₃)₂ (7.4 mg, 0.05 eq.), diisopropylamine (0.1 mL, 2.00 eq.) and ethynylferrocene (52.0 mg, 0.25 mmol, 1.20 eq.) dissolved in 25 ml THF. Red solid (101 mg, 0.19 mmol, 92 %).

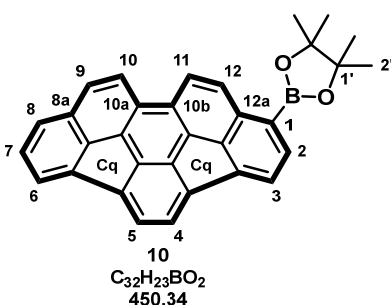
¹H NMR (500 MHz, C₂D₂Cl₄) δ = 8.12 (d, *J* = 8.8 Hz, 1H, *H11*), 8.06 (d, *J* = 8.7 Hz, 1H, *H10*), 8.01 (d, *J* = 8.8 Hz, 1H, *H12*), 7.76 (d, *J* = 8.7 Hz, 1H, *H9*), 7.67 (d, *J* = 7.0 Hz, 1H, *H6*), 7.63 – 7.57 (m, 4H, *H3* + *H4* + *H5* + *H8*), 7.51 (d, *J* = 7.3 Hz, 1H, *H2*), 7.36 (dd, *J* = 8.1, 7.0 Hz, 1H, *H7*), 4.58 (t, *J* = 1.8 Hz, 2H, *H2'*), 4.27 (t, *J* = 1.8 Hz, 2H, *H3'*), 4.25 (s, 5H, *H4'*); ¹³C NMR (125 MHz, C₂D₂Cl₄) δ = 138.66 (*Cq*), 138.64(*Cq*), 138.18 (*Cq*), 138.16 (*Cq*), 138.05 (*Cq*), 137.97 (*Cq*), 137.94 (*Cq*), 137.79 (*Cq*), 136.44 (*Cq*), 136.38 (*Cq*), 132.21 (*C2*), 130.14 (*C10b*), 129.71 (*C10a*), 129.08 (*C12a*), 128.97 (*C8a*), 128.93 (*C7*), 127.01 (*C9*), 126.82 (*C8*), 125.72 (*C5*), 125.64 (*C4*), 125.58 (*C12*), 124.36 (*C11*), 123.93 (*C10*), 123.65 (*C6*), 123.44 (*C3*), 121.68 (*C1*), 95.04 (*Cac2*), 83.35 (*Cac1*), 71.69 (2*C*, *C2'*), 70.13 (5*C*, *C4'*), 69.30 (2*C*, *C3'*), 64.74 (*C1'*); IR (cm⁻¹) 2958, 2875, 1463, 1382, 1149, 956, 801 752, 739; MS (EI): *m/z* (*rel. int.*) = 532 (100 %), 323 (40 %); HRMS (EI) *m/z* Calcd for C₃₈H₂₀Fe [M]⁺: 532.0914. Found: 532.0921.



4-Ferrocenyl-13,16-difluorobenzo[s]picene (5) was synthesized by adding to a solution of Pd(PPh₃)₄ (97.0 mg, 0.08 mmol, 0.05 eq.) and cesium fluoride (168 mg, 1.11 mmol, 2.2 eq.) in dry DMF (2 mL), tri-*n*-butylstannylferrocene (250 mg, 0.53 mmol, 1.0 eq.), a suspension of **Idpc-Br** (250 mg, 0.56 mmol, 1.1 eq.) in dry DMF (9 mL), and copper(I)iodide (45.0 mg, 0.24 mmol, 0.5 eq.). The reaction mixture was

heated at 50 °C for 15 h whilst monitoring the reaction via EI-MS until full consumption of starting material. Upon cooling to room temperature the reaction mixture was filtered over a short celite plug with ethyl acetate (150 mL). The filtrate was washed with bicarbonate solution (2 x 30 mL), water (2 x 30 mL) and brine (30 mL), dried over magnesium sulfate, filtered and concentrated under reduced pressure. Column chromatography on silica using PE/ethyl acetate = 9:1 as eluent yielded a deep red powder. Repeated washing with copious amounts of *n*-pentane yielded title compound **5** as red powder (200 mg, 0.37 mmol, 65 %). Crystals suitable for X-ray diffraction were grown by slow diffusion of *n*-pentane into a concentrated solution of **5** in CH₂Cl₂.

¹H NMR (800 MHz, CDCl₃) δ = 8.75 (d, ³J_{HH} = 9.1 Hz, 1H, **H5**), 8.52 (d, ³J_{HH} = 8.8 Hz, 1H, **H7**), 8.47 (d, ³J_{HH} = 9.1 Hz, 1H, **H6**), 8.23 (dd, ⁶J_{HF} (through space) = 13.8 Hz, ³J_{HH} = 8.2 Hz, 1H, **H12**), 8.11 (dd, ⁶J_{HF} (through space) = 13.0 Hz, ³J_{HH} = 7.7 Hz, 1H, **H1**), 8.11 (d, ³J_{HH} = 8.7 Hz, 1H, **H8**), 7.97 (d, ³J_{HH} = 7.9 Hz, 1H, **H9**), 7.93 (d, ³J_{HH} = 7.7 Hz, 1H, **H3**), 7.61 (dd, ³J_{HH} = 8.2 Hz, 7.0 Hz, 1H, **H11**), 7.59 (dd, ³J_{HH} = 7.9 Hz, 7.0 Hz, 1H, **H10**), 7.54 (dd, ³J_{HH} = 9.1 Hz, 7.7 Hz, 1H, **H2**), 7.39 (d, ³J_{HH} = 7.4 Hz, 1H, **H14**), 7.38 (d, ³J_{HH} = 7.4 Hz, 1H, **H15**), 4.74 (s, 2H, **H2'** + **H5'**), 4.49 (s, 2H, **H3'** + **H4'**), 4.30 (s, 5H, **H6'**); **¹⁹F NMR** (376 MHz, CDCl₃) δ = -104.07 (d, ⁵J_{FF} = 17.7 Hz, 1F, **F16**), -104.20 (d, ⁵J_{FF} = 17.7 Hz, 1F, **F13**); **¹³C NMR** (200 MHz, CDCl₃) δ = 155.34 (dd, ¹J_{CF} = 246.2 Hz, ⁴J_{CF} = 1.8 Hz, **C13**), 155.31 (dd, ¹J_{CF} = 250.2 Hz, ⁴J_{CF} = 1.7 Hz, **C16**), 135.55 (**C4**), 132.47 (**C8a**), 131.03 (**C4a**), 130.77 (d, ⁴J_{CF} = 3.2 Hz, **C16c**), 130.35 (d, ⁴J_{CF} = 3.1 Hz, **C12a**), 130.06 (**C6b**), 129.83 (d, ⁵J_{CF} (through space) = 14.4 Hz, **C12**), 129.82 (**C6a**), 129.51 (**C8**), 128.83 (d, ⁵J_{CF} (through space) = 14.2 Hz, **C1**), 128.40 (**C3**), 127.64 (**C5**), 127.29 (**C9**), 126.26 (**C10**), 125.36 (**C11**), 124.54 (**C3**), 123.74 (d, ³J_{CF} = 3.0 Hz, **C12b**), 123.53 (d, ³J_{CF} = 3.1 Hz, **C16b**), 120.54 (dd, ²J_{CF} = 13.7 Hz, ³J_{CF} = 2.0 Hz, **C12c**), 120.27 (dd, ²J_{CF} = 14.0 Hz, ³J_{CF} = 2.5 Hz, **C16a**), 119.89 (**C8**), 119.37 (**C6**), 114.46 (dd, ²J_{CF} = 11.8 Hz, ³J_{CF} = 9.6 Hz, **C14**), 114.32 (dd, ²J_{CF} = 12.2 Hz, ³J_{CF} = 10.0 Hz, **C15**), 87.98 (**C1'**), 71.95 (**C5'**), 70.46 (**C2'**), 70.18 (5C, **C6'**), 68.69 (2C, **C3'+4'**); **MS** (EI): *m/z* (rel. int.) = 548. (100 %), 363 (80 %).

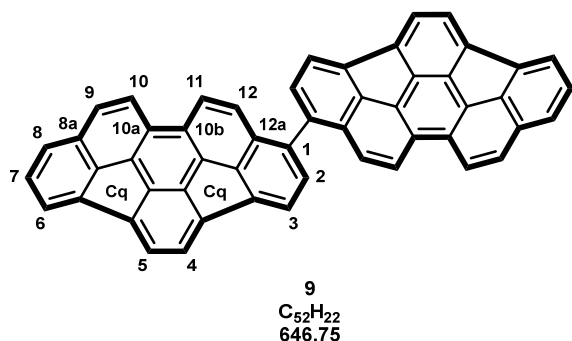


Idpc-B(pin) (10) was synthesized using **Idpc-Br** (100 mg, 0.25 mmol, 1.00 eq.), Pd(dppf)Cl₂ (10.0 mg, 0.01 mmol, 0.05 eq.), potassium acetate (73.0 mg, 0.74 mmol, 3.00 eq.), and bis(pinacolato)diboron (94.5 mg, 0.37 mmol, 1.50 eq.) dissolved in dry 1,4-dioxane (60 mL). The mixture was heated under reflux until full consumption of starting materials (TLC). The volatiles were removed under reduced pressure and water (200 mL) was added to

the crude. The resulting mixture was extracted with CH₂Cl₂ (3 x 100 mL). The organic phases were dried over magnesium sulfate, filtered, and the solvent was removed under reduced pressure. The crude product was purified by column chromatography on silica using a gradient system consisting of initially PE/CH₂Cl₂ = 3:1 gradually changed to CH₂Cl₂ as eluent to obtain boronic acid pinacol ester **10** as an orange solid (101 mg, 0.22 mmol, 90 %).

¹H NMR (400 MHz, CDCl₃): δ = 8.48 (d, ³J_{HH} = 8.9 Hz, 1H), 8.13 (d, ³J_{HH} = 8.9 Hz, 1H), 8.12 (d, ³J_{HH} = 8.7 Hz, 1H), 7.98 (d, ³J_{HH} = 6.9 Hz, 1H), 7.78 (d, ³J_{HH} = 8.8 Hz, 1H), 7.71 (d, ³J_{HH} = 6.9 Hz, 2H), 7.67 – 7.66 (m, 2H), 7.65 (d, ³J_{HH} = 8.2 Hz, 1H), 7.39 (dd, ³J_{HH} = 8.2, 6.9 Hz, 1H), 1.44 (s, 12H); **¹³C**

NMR (100 MHz, CDCl₃) δ = 141.91, 139.40, 139.06, 138.61, 138.59, 138.41, 138.18, 137.97, 136.94, 136.47, 133.04, 130.25, 130.07, 129.16, 128.78, 128.68, 126.92, 126.88, 125.91, 125.43, 124.19, 124.15, 123.57, 122.70, 83.97, 25.16; **IR** (cm⁻¹) 2981, 1697, 1594, 1507, 1422, 1341, 1143, 1106, 1061, 954, 807, 783, 753, 703; **MS** (EI): m/z (*rel. int.*) = 450 (100 %), 323 (60 %).



1,1'-Bisindacenopencene (Idpc)₂ (9) was synthesized according to general procedure A using **Idpc-Br** (23.0 mg, 0.06 mmol, 1.00 eq.), Pd(PPh₃)₄ (1.0 mg, 0.01 eq.), sodium carbonate (24.0 mg, 0.22 mmol, 3.00 eq.) and boronic acid pinacol ester **10** in a 1,4-dioxane/H₂O (14:1) solution (50 mL). (30.0 mg, 0.07 mmol, 1.2 eq.) Red solid (21.5 mg, 0.03 mmol, 60 %).

¹H NMR (600 MHz, C₂D₂Cl₄): δ = 8.05 (d, ³J_{HH} = 8.6 Hz, 1H, **H10**), 7.99 (d, ³J_{HH} = 8.8 Hz, 1H, **H11**), 7.83 (d, ³J_{HH} = 6.9 Hz, 2H, **H3**), 7.75 (d, ³J_{HH} = 8.6 Hz, 2H, **H9**), 7.73 – 7.67 (m, 8H, **H4** + **H5** + **H6** + **H12**), 7.62 (d, ³J_{HH} = 8.1 Hz, 2H, **H8**), 7.52 (d, ³J_{HH} = 6.9 Hz, 2H, **H2**), 7.38 (t, ³J_{HH} = 7.5 Hz, 2H, **H7**); **¹³C NMR** (150 MHz, C₂D₂Cl₄) δ = 138.79 (**Cq**), 138.67 (**Cq**), 138.54 (**Cq**), 138.29 (**Cq**), 138.25 (**Cq**), 138.13 (**Cq**), 138.07 (**Cq**), 137.95 (**Cq**), 137.46 (**CI'**), 136.94 (**Cq**), 136.48 (**Cq**), 130.69 (**C2**), 129.95 (**CI0b**), 129.76 (**CI0a**), 128.98 (**C8a**), 128.96 (**C7**), 128.28 (**CI2a**), 127.02 (**C9**), 126.83 (**C8**), 126.50 (**CI2**), 125.80 (**C5**), 125.69 (**C4**), 124.21 (**CI1**), 123.84 (**CI0**), 123.68 (**C6**), 123.67 (**C3**); **IR** (cm⁻¹) 3029, 2891, 2202, 1869, 1591, 1504, 1415, 1375, 1339, 1250, 1132, 1107, 951, 892, 852, 801, 780, 757, 704, 667; **MS** (EI): m/z (*rel. int.*) = 646 (100 %), 323 (50 %).

Supporting information

Detailed information about X-ray diffraction studies, quantum chemical calculations, Uv/vis and luminescence spectroscopy as well as graphical representations of all spectra and cyclic voltammograms are to be found in the ESI.

Conflict of interest

There are no conflicts to declare.

Acknowledgement

The authors thank Anke Friemel und Ulrich Haunz of the NMR-core facility of the University of Konstanz for support with the NMR measurements and Dr. Inigo Göttker gen. Schnetmann and Bernhard Weibert for support with the X-ray diffraction studies. We wish to thank Dr. Gerald Dräger (University of Hannover, Institut für Organische Chemie) for HRMS measurements. Financial support by the DFG-project Wi 1262/10-2 is gratefully acknowledged.

References

- [1] W. E. Barth, R. G. Lawton, *J. Am. Chem. Soc.* **1966**, *88*, 380-381.
- [2] J. Dey, A. Y. Will, R. A. Agbaria, P. W. Rabideau, A. H. Abdourazak, R. Sygula, I. M. Warner, *J. Fluoresc.* **1997**, *7*, 231-236.
- [3] M. Yamada, K. Ohkubo, M. Shionoya, S. Fukuzumi, *J. Am. Chem. Soc.* **2014**, *136*, 13240-13248.
- [4] M. Yamaji, K. Takehira, T. Mikoshiba, S. Tojo, Y. Okada, M. Fujitsuka, T. Majima, S. Tobita, J. Nishimura, *Chem. Phys. Lett.* **2006**, *425*, 53-57.
- [5] Y.-L. Wu, M. C. Stuparu, C. Boudon, J.-P. Gisselbrecht, W. B. Schweizer, K. K. Baldrige, J. S. Siegel, F. Diederich, *J. Org. Chem.* **2012**, *77*, 11014-11026.
- [6] R. C. Haddon, *Science* **1993**, *261*, 1545-1550.
- [7] Z. Lin, C. Li, D. Meng, Y. Li, Z. Wang, *Chem.--Asian J.* **2016**, *11*, 2695-2699.
- [8] A. S. Filatov, L. T. Scott, M. A. Petrukhina, *Cryst. Growth Des.* **2010**, *10*, 4607-4621.
- [9] R. C. Haddon, R. E. Palmer, H. W. Kroto, P. A. Sermon, H. W. Kroto, A. L. Mackay, G. Turner, D. R. M. Walton, *Philos. Trans. R. Soc. London, Ser. A* **1993**, *343*, 53-62.
- [10] C. Bruno, R. Benassi, A. Passalacqua, F. Paolucci, C. Fontanesi, M. Marcaccio, E. A. Jackson, L. T. Scott, *J. Phys. Chem. B* **2009**, *113*, 1954-1962.
- [11] G. Valenti, C. Bruno, S. Rapino, A. Fiorani, E. A. Jackson, L. T. Scott, F. Paolucci, M. Marcaccio, *J. Phys. Chem. C* **2010**, *114*, 19467-19472.
- [12] V. M. Tsefrikas, L. T. Scott, *Chem. Rev.* **2006**, *106*, 4868-4884.
- [13] L. T. Scott, *Chem. Soc. Rev.* **2015**, *44*, 6464-6471.
- [14] V. Rajeshkumar, Y. T. Lee, M. C. Stuparu, *Eur. J. Org. Chem.* **2016**, *2016*, 36-40.
- [15] J. Li, A. Terec, Y. Wang, H. Joshi, Y. Lu, H. Sun, M. C. Stuparu, *J. Am. Chem. Soc.* **2017**, *139*, 3089-3094.
- [16] E. Nestoros, M. C. Stuparu, *Chem. Commun.* **2018**, *54*, 6503-6519.
- [17] D. Halilovic, M. Budanović, Z. R. Wong, R. D. Webster, J. Huh, M. C. Stuparu, *J. Org. Chem.* **2018**, *83*, 3529-3536.
- [18] E. M. Muzammil, D. Halilovic, M. C. Stuparu, *Commun. Chem.* **2019**, *2*, 58.
- [19] L. Wang, P. B. Shevlin, *Org. Lett.* **2000**, *2*, 3703-3705.

- [20] K. Y. Amsharov, P. Merz, *J. Org. Chem.* **2012**, *77*, 5445-5448.
- [21] K. Y. Amsharov, M. A. Kabdulov, M. Jansen, *Angew. Chem., Int. Ed.* **2012**, *51*, 4594-4597.
- [22] S. N. Spisak, J. Li, A. Y. Rogachev, Z. Wei, O. Papaianina, K. Amsharov, A. V. Rybalchenko, A. A. Goryunkov, M. A. Petrukhina, *Organometallics* **2016**, *35*, 3105-3111.
- [23] O. Papaianina, V. A. Akhmetov, A. A. Goryunkov, F. Hampel, F. W. Heinemann, K. Y. Amsharov, *Angew. Chem., Int. Ed.* **2017**, *56*, 4834-4838.
- [24] F. B. Mallory, C. S. Wood, J. T. Gordon, *J. Am. Chem. Soc.* **1964**, *86*, 3094-3102.
- [25] D. E. Fagnani, A. Sotuyo, R. K. Castellano, in *Comprehensive Supramolecular Chemistry II* (Ed.: J. L. Atwood), Elsevier, Oxford, **2017**, pp. 121-148.
- [26] *1,8-Dimethyl Idpc (CSD code WUDNOY) lacks 3D-coordinates in the CSD database 2020.*
- [27] L. Venkataraman, J. E. Klare, C. Nuckolls, M. S. Hybertsen, M. L. Steigerwald, *Nature* **2006**, *442*, 904-907.
- [28] D. Vonlanthen, A. Mishchenko, M. Elbing, M. Neuburger, T. Wandlowski, M. Mayor, *Angew. Chem., Int. Ed.* **2009**, *48*, 8886-8890.
- [29] A. Sygula, S. Saebø, *Int. J. Quantum Chem.* **2009**, *109*, 65-72.
- [30] R. C. Haddon, L. T. Scott, *Pure Appl. Chem.* **1986**, *58*, 137 - 142.
- [31] C. S. Jones, E. Elliott, J. S. Siegel, *Synlett* **2004**, *2004*, 187-191.
- [32] P. Bachawala, T. Ratterman, N. Kaval, J. Mack, *Tetrahedron* **2017**, *73*, 3831-3837.
- [33] Y.-T. Wu, D. Bandera, R. Maag, A. Linden, K. K. Baldrige, J. S. Siegel, *J. Am. Chem. Soc.* **2008**, *130*, 10729-10739.
- [34] G. H. Grube, E. L. Elliott, R. J. Steffens, C. S. Jones, K. K. Baldrige, J. S. Siegel, *Org. Lett.* **2003**, *5*, 713-716.
- [35] B. Topolinski, B. M. Schmidt, S. Schwagerus, M. Kathan, D. Lentz, *Eur. J. Inorg. Chem.* **2014**, *2014*, 5391-5405.
- [36] B. Topolinski, B. M. Schmidt, M. Kathan, S. I. Troyanov, D. Lentz, *Chem. Commun.* **2012**, *48*, 6298-6300.
- [37] J. C. Hanson, C. E. Nordman, *Acta Crystallogr., Sect. B: Struct. Sci.* **1976**, *32*, 1147-1153.
- [38] A. Sygula, H. E. Folsom, R. Sygula, A. H. Abdourazak, Z. Marcinow, F. R. Fronczek, P. W. Rabideau, *J. Chem. Soc., Chem. Commun.* **1994**, 2571-2572.
- [39] B. D. Steinberg, E. A. Jackson, A. S. Filatov, A. Wakamiya, M. A. Petrukhina, L. T. Scott, *J. Am. Chem. Soc.* **2009**, *131*, 10537-10545.
- [40] Y.-T. Wu, T. Hayama, K. K. Baldrige, A. Linden, J. S. Siegel, *J. Am. Chem. Soc.* **2006**, *128*, 6870-6884.
- [41] A. K. Dutta, A. Linden, L. Zoppi, K. K. Baldrige, J. S. Siegel, *Angew. Chem., Int. Ed.* **2015**, *54*, 10792-10796.
- [42] S. Lampart, L. M. Roch, A. K. Dutta, Y. Wang, R. Warshamanage, A. D. Finke, A. Linden, K. K. Baldrige, J. S. Siegel, *Angew. Chem., Int. Ed.* **2016**, *55*, 14648-14652.
- [43] B. Topolinski, B. M. Schmidt, S. Higashibayashi, H. Sakurai, D. Lentz, *Dalton Trans.* **2013**, *42*, 13809-13812.
- [44] S. Fery-Forgues, B. Delavaux-Nicot, *J. Photochem. Photobiol., A* **2000**, *132*, 137-159.
- [45] A. Kasprzak, A. Kowalczyk, A. Jagielska, B. Wagner, A. M. Nowicka, H. Sakurai, *Dalton Trans.* **2020**, *49*, 9965-9971.
- [46] T. Wombacher, R. Goddard, C. W. Lehmann, J. J. Schneider, *Chem. Commun.* **2017**, *53*, 7030-7033.
- [47] V. Barát, M. Budanović, D. Halilovic, J. Huh, R. D. Webster, S. H. Mahadevegowda, M. C. Stuparu, *Chem. Commun.* **2019**, *55*, 3113-3116.
- [48] A. A. K. Karunathilake, C. M. Thompson, S. Perananthan, J. P. Ferraris, R. A. Smaldone, *Chem. Commun.* **2016**, *52*, 12881-12884.
- [49] M. Krejčík, M. Danek, F. Hartl, *J. Electroanal. Chem.* **1991**, *317*, 179-187.
- [50] M. Baumgarten, L. Gherghel, M. Wagner, A. Weitz, M. Rabinovitz, P.-C. Cheng, L. T. Scott, *J. Am. Chem. Soc.* **1995**, *117*, 6254-6257.
- [51] D. M. D'Alessandro, F. R. Keene, *Chem. Soc. Rev.* **2006**, *35*, 424-440.
- [52] M. J. Frisch, G. W. Trucks, H. B. Schlegel, G. E. Scuseria, M. A. Robb, J. R. Cheeseman, G. Scalmani, V. Barone, G. A. Petersson, H. Nakatsuji, X. Li, M. Caricato, A. V. Marenich, J. Bloino, B. G. Janesko, R. Gomperts, B. Mennucci, H. P. Hratchian, J. V. Ortiz, A. F. Izmaylov, J. L. Sonnenberg, Williams, F. Ding,

- F. Lipparini, F. Egidi, J. Goings, B. Peng, A. Petrone, T. Henderson, D. Ranasinghe, V. G. Zakrzewski, J. Gao, N. Rega, G. Zheng, W. Liang, M. Hada, M. Ehara, K. Toyota, R. Fukuda, J. Hasegawa, M. Ishida, T. Nakajima, Y. Honda, O. Kitao, H. Nakai, T. Vreven, K. Throssell, J. A. Montgomery Jr., J. E. Peralta, F. Ogliaro, M. J. Bearpark, J. J. Heyd, E. N. Brothers, K. N. Kudin, V. N. Staroverov, T. A. Keith, R. Kobayashi, J. Normand, K. Raghavachari, A. P. Rendell, J. C. Burant, S. S. Iyengar, J. Tomasi, M. Cossi, J. M. Millam, M. Klene, C. Adamo, R. Cammi, J. W. Ochterski, R. L. Martin, K. Morokuma, O. Farkas, J. B. Foresman, D. J. Fox, Gaussian 16 Rev. C.01. Wallingford, CT, 2016.
- [53] M. Cossi, N. Rega, G. Scalmani, V. Barone, *J. Comput. Chem.* **2003**, *24*, 669-681.
- [54] M. Dolg, U. Wedig, H. Stoll, H. Preuss, *J. Chem. Phys.* **1987**, *86*, 866-872.
- [55] P. C. Hariharan, J. A. Pople, *Theor. Chim. Acta* **1973**, *28*, 213-222.
- [56] J. P. Perdew, K. Burke, M. Ernzerhof, *Phys. Rev. Lett.* **1996**, *77*, 3865-3868.
- [57] C. Adamo, V. Barone, *J. Chem. Phys.* **1999**, *110*, 6158-6170.
- [58] N. M. O'Boyle, A. L. Tenderholt, K. M. Langner, *J. Comput. Chem.* **2008**, *29*, 839-845.
- [59] M. D. Hanwell, D. E. Curtis, D. C. Lonie, T. Vandermeersch, E. Zurek, G. R. Hutchison, *J. Cheminf.* **2012**, *4*, 17.
- [60] O. Tange, ;login: *The USENIX Magazine* **2011**, *36*, 42-47.
- [61] W. Humphrey, A. Dalke, K. Schulten, *J. Mol. Graphics* **1996**, *14*, 33-38.
- [62] POV-Ray - The Persistence of Vision Raytracer. <http://www.povray.org/download/>.
- [63] W. L. F. Armarego, C. L. L. Chai, *Purification of Laboratory Chemicals*, 5th ed., Elsevier, Amsterdam, **2003**.